NASA
Technical
Paper
2525

July 1986

NASA-TP-2525 19860018448

Analytical Techniques of Pilot Scanning Behavior and Their Application

Randall L. Harris, Sr.,
Bobby J. Glover, and
Amos A. Spady, Jr.

NASA

Analytical Techniques of Pilot Scanning Behavior and Their Application

Randall L. Harris, Sr.
*Langley Research Center
Hampton, Virginia*

Bobby J. Glover
*PRC Kentron, Inc.
Hampton, Virginia*

Amos A. Spady, Jr.
*Langley Research Center
Hampton, Virginia*

Contents

Summary

This report documents the state of the art of oculometric data analysis techniques and their applications in certain research areas such as pilot workload, information transfer from displays to pilots, strategy and role of pilots, and pilot training. The analysis techniques result in the following data: real-time viewing of the pilot's scanning behavior, average dwell times, dwell percentages, instrument transition paths, dwell histograms, and entropy rate measures. Visual workload estimates are obtained from dwell percentages and entropy rate measures. Information transfer evaluations are performed primarily with average dwell times, dwell histograms, and entropy rates. Pilot strategy and role are determined by using scan time histories, time-locked time histories, and transition matrix data. Pilot training evaluations use real-time scanning data and entropy rate measures. Overviews of the experimental setup, data analysis techniques, and software are presented. Several results from these techniques are discussed. A glossary of terms frequently used in pilot scanning behavior and a bibliography of reports on related research sponsored by NASA Langley Research Center are presented.

Introduction

Man-machine flight research at Langley Research Center (LaRC) addresses human factors problems such as the effects of a particular type of instrument on pilot workload, the effects of a new instrument on pilot strategy, the effects of a new procedure on pilot role, and the effects of data format on information transfer. To investigate these problems, a research program was initiated to develop experimental protocols and techniques for analyzing data on pilot scanning behavior.

The measurement of pilot scanning behavior began in 1946 when Jones et al. (ref. 1) determined a pilot's lookpoint by subjectively judging motion picture frames of a pilot's face. The outcome of this early research was the development of an instrument placement standard (namely, "the standard six") and shape-coding for control knobs. The results of that work are still being used as design standards and can be found in a number of handbooks (e.g., ref. 2). The results were also responsible for the FAA's regulations concerning the basic "T" arrangement of electromechanical instruments (ref. 3). These design standards, which are still being applied today, are helpful, but they may not be sufficient for designing current and future aircraft cockpit displays.

With the advent of the oculometer, progress has been made in the past decade in the development of the necessary scanning-behavior analysis techniques, coupled with their correlation to control inputs and aircraft parameters, to evaluate display design. In the past it had been erroneously assumed that if dwell times and scanning sequences could be quantified, then a better display could be designed. These scanning-behavior measures by themselves do not provide sufficient information for the optimal design of a display. Today, with the aid of oculometer hardware and software, determining in real time where a pilot is looking can be done to an accuracy of 1 visual degree (a circle 0.5 in. in diameter). These data are recorded in a computer-compatible format 30 times per second along with other pertinent aircraft and performance measurements. The oculometer hardware has been developed and miniaturized to the point that it can be placed in most aircraft simulator cockpits. For the past 10 years, NASA has been developing analytical tools which when applied to pilot scanning-behavior data will give measurements that can be used to interpret pilot workload, to determine relative rates of information transfer from displays to pilots, to determine pilot strategy and/or role, and to assist in pilot training.

The purpose of this report is to review the techniques developed at LaRC for analyzing data on pilot scanning behavior and to show how these techniques can be applied to the human factors research areas mentioned above. Four appendices are included in the report. Appendix A, written by Daniel W. Burdette of PRC Kentron, Inc., describes the evolution of LaRC's oculometer system over the past several years as well as procedures for its setup and calibration. Appendix B provides a functional description of three computer programs which have been developed to analyze data on pilot scanning behavior. Appendix C is a glossary of frequently used terms in scanning behavior. Appendix D is a bibliography on scanning-behavior research sponsored by LaRC.

Symbols and Abbreviations

|	
AC	alternating current
ADF	automatic direction finder
AGL	above ground level
AS	airspeed indicator
BA	barometric altimeter
CMD	command
D	number of off-diagonal terms in transition matrix
DT	average dwell time
EADI	electronic attitude direction indicator

EHSI	electronic horizontal situation indicator
FD	flight director
GSI	glide slope indicator
H	average entropy
$\dot{H}$	entropy rate
HSI	horizontal situation indicator
ILS	instrument landing system
N	number of instruments
P	dwell percentage
P_{ij}	two-way transition percentage between instruments i and j
p	probability
RA	radar altimeter
TD	task demand
VSI	vertical speed indicator
x	element in a matrix

Subscripts:

i	"from" instrument
j	"to" instrument

Anaytical Procedures

The analysis techniques which have been developed to analyze pilot scanning behavior are presented in four sections. The first section describes qualitative evaluations of the pilot's lookpoint on the instrument panel. The second section describes the somewhat traditional quantitative analysis of time histories, time-locked time histories, transition matrices, and statistical tests of scanning-behavior measures. The third and fourth sections describe more advanced quantitative analysis techniques of dwell histograms and measurement of scanning randomness. Other analysis tools, based upon the authors' experience, that could be developed are proposed in a fifth section.

Real-Time Viewing of Lookpoint

A very simple method of analyzing scanning behavior is observing the video of the instrument panel scene with the pilot's instantaneous lookpoint superimposed upon it. Figure 1 is a composite photograph showing the measurement equipment, the pilot flying a simulator, and the type of video presentation available to the researcher conducting the tests. Viewing
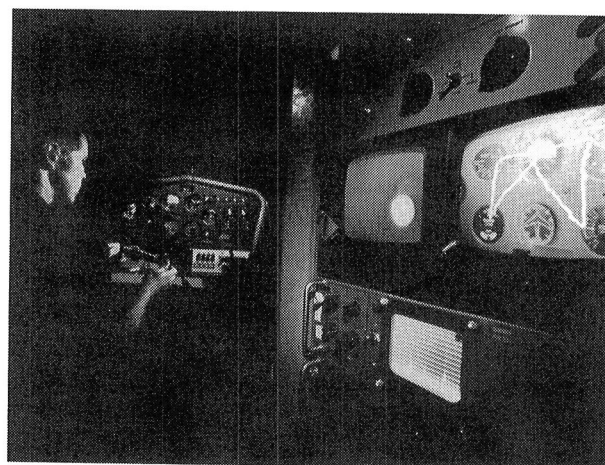
Figure 1. Oculometer setup with real-time view of subject's lookpoint.

the instantaneous lookpoint can be done in real time during simulated or actual flight or from a video tape after the testing session is over. Observing the pilot's lookpoint as it moves from instrument to instrument enables the researcher to quickly develop an impression of the pilot's scanning behavior. In addition, viewing the lookpoint provides some appreciation of the quality of the data being collected during the experimental sessions. For example, the researcher can detect consistent dwells skewed off the instrument faces indicating poor calibration, or he may observe extended "out-of-track" periods indicating that certain parameters should be checked and/or readjusted. (See appendix A.) The real-time video also provides the operator with information needed to assure that the oculometer system is operating correctly. For example, if the system is out of track for extended periods of time, then certain oculometer system parameters should be checked.

Traditional Scanning-Behavior Analysis

One of the first questions asked about a pilot's scanning behavior in many circumstances is, how much time does a pilot spend on the various instruments? The software required for providing the answer would seem to be quite straightforward and simple. However, it can be quite complex, depending upon the type of scanning-behavior statistics that are calculated and the sophistication of the algorithm used to determine fixations. The data analyses presented here include time histories, time-locked time histories, transition matrices, and statistical tests such as the t test and the F ratio.

Time histories. A simple method of exploring the question of where a pilot looks can be answered by a
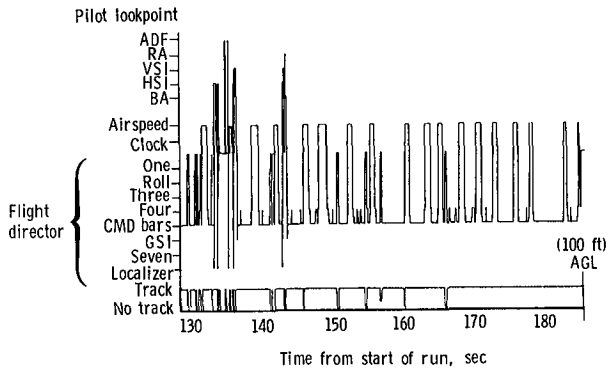
Figure 2. Time histories of one pilot's scan during landing
approach (altitude of 700 to 100 ft above ground level).

Figure 3. Time-locked time history at a given sample time
relative to a triggering event.

time history plot of the lookpoint. A typical time history is shown in figure 2. The ordinate is scaled in divisions representing the different instruments. Time is plotted along the abscissa. This technique, like real-time viewing, permits a subjective evaluation of the scanning behavior by allowing the researcher to see the entire run in one view and thereby identify some candidate measures for scanning behavior, such as (1) the number of times a pilot looks out of the window on a landing approach, (2) the number of times a pilot looks at the engine instruments on takeoff, (3) the number of blinks per minute, or (4) the total number of transitions between any particular pair of instruments. Particular analytical evaluation procedures can then be incorporated into computer programs, and in turn, the reduced data can be used for more detailed evaluation by the experimenter.

Time-locked time histories. It is useful to know how a pilot responds to various tasks which he must perform. One recently developed analysis technique involves time locking the scanning analysis to some event, such as performing a secondary task. This technique is similar to that used in the analysis of evoked brain potentials in reference 4, where the amplitudes of the brain waves at specified times from the beginning of triggering events are averaged. A time history is produced in which the ordinate values represent the average amplitude and the abscissa is the time with respect to the triggering event. In this scanning-behavior analysis procedure, however, the percent of time looking at each instrument at specified times relative to triggering events (for example, a beep) is calculated. A time-locked time history of these dwell percentages is produced in which the ordinate values represent the percent of time spent on each instrument and the abscissa is the time with respect to the triggering event. Figure 3 illustrates in bar graph form what the plot would look like at a given sample time relative to the triggering event.
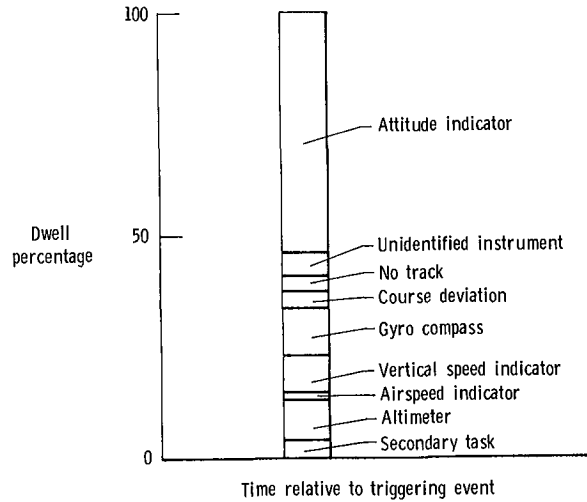
These percentage values are obtained by adding lookpoints which occurred at the same time relative to many occurrences of the same triggering event. The height of each bar is proportional to the dwell percentage of the appropriate instrument at a time relative to the triggering event. For example, the dwell percentage on the attitude indicator in figure 3 would be approximately 55 percent. By plotting all the instruments in the same relative vertical positions and placing all the oculometer samples side by side, a time history is formed. (See fig. 4.)
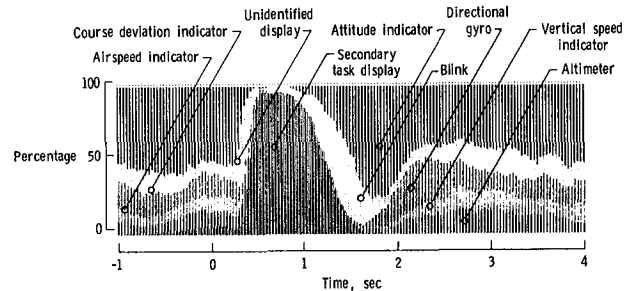
Figure 4. Time-locked time history.

Figure 4 shows data collected during tests to determine the dwell times necessary to accomplish specific information-gathering tasks. The dwell time taken by a pilot to classify the up or down position of a display needle whenever a beep sounded was determined. The time history was time locked to a beep (time zero) that signaled the start of the secondary task. In this figure each instrument is represented by a different shading. The time interval corresponds to the sampling rate of the oculometer (30 samples per second). As seen in the figure, about one third of a second after the beep, the beginning of the transition to the side task is initiated (increase in

percentage of time on the side task). The first event after the look at and response to the side task is a blink (as indicated by the momentary loss of track by the oculometer), followed by a look at the attitude indicator, then the directional gyro (both indicated by increases in the percentage of time looking at these instruments). Events that are naturally occurring in a simulation (e.g., pressing of a particular button by a pilot, a sound from the master caution and warning system, or receipt of a certain instruction from air traffic control) could be used to trigger the data instead of a contrived beep.

Transition matrices. The transition matrix describes the probability of transitioning from one instrument to another and can be thought of as a second-order Markov transition matrix. Each element of the transition matrix is the total number of one thirtieths of a second that the pilot looked at an instrument during an oculometer sample period, given that he was looking at some other or the same instrument during the previous oculometer sample. These matrices are used to quantify the time a pilot spends on the various instruments and the patterns of his eye movements. These measures include average dwell times, instrument dwell percentages, and one-way or two-way transitions (see appendix C) and can be quite useful when performing exploratory or descriptive research tests.

For the situation of three instruments, the transition matrix would be as follows:

"To" instrument number, j

$$\text{"From" instrument number, } i \quad \begin{array}{c} \\ 1 \\ 2 \\ 3 \end{array} \begin{array}{ccc} 1 & 2 & 3 \\ \left[\begin{array}{ccc} x_{11} & x_{12} & x_{13} \\ x_{21} & x_{22} & x_{23} \\ x_{31} & x_{32} & x_{33} \end{array}\right] \end{array}$$

The first subscript to the matrix element represents the "from" instrument, (i), and the second subscript represents the "to" instrument, (j). The result after analyzing a set of data is that each x_{ij} has the value of the number of times the transition from instrument i to instrument j occurred. The magnitudes of the diagonal elements are the largest, since more time is spent looking at an instrument (transitions to the same instrument) than is spent transitioning to new instruments. From the data in this matrix, several measures can be calculated.

Average dwell time of each instrument can be obtained by summing the elements of each column and dividing by the total number of transitions to that instrument (sum of the off-diagonal terms in that column) and converting the quotient to seconds

by dividing by the sampling rate of the oculometer (30 samples per second). The average dwell time for instrument j, $(\text{DT})_j$, would be

$$(\text{DT})_j = \frac{\sum_{i=1}^{N} x_{ij} / \sum_{\substack{i=1 \\ i \neq j}}^{N} x_{ij}}{30}$$

where N is the number of instruments.

The dwell percentage on each instrument can be calculated by dividing the sum of each column by the total sum of all the elements. For instrument j in the above example, the dwell percentage, P_j, would be

$$P_j = \frac{\sum_{i=1}^{N} x_{ij}}{\sum_{i=1}^{N} \sum_{j=1}^{N} x_{ij}}$$

Finally, the occurrence of a specific one-way transition as a percentage of all one-way transitions can be calculated by dividing the appropriate off-diagonal element by the sum of all the off-diagonal elements. Two-way transition percentages, that is transition percentage from instrument 1 to 2 (x_{12}) and from instrument 2 to 1 (x_{21}), can be obtained by summing the appropriate off-diagonal elements (i.e., x_{12} and x_{21}) and dividing by the sum of the off-diagonal terms. Thus, the two-way transition percentage, P_{12}, between instruments 1 and 2 would be

$$P_{12} = \frac{x_{12} + x_{21}}{\sum_{i=1}^{N} \sum_{\substack{j=1 \\ j \neq i}}^{N} x_{ij}}$$

Graphs showing these transition matrix measures are shown in figures 5 and 6. These figures are airline pilots' scans during an instrument landing approach (ref. 5). To assist in the interpretation of the data, these graphs approximate the placement and shape of instruments on the instrument panel. Generally, the instruments are thought of as round, since their faces are circular, even though the outside bezel is almost square. Inside the outline of each instrument are the dwell percentage, rounded off to the nearest percent or tenth of a percent, and the average dwell time, rounded off to the nearest tenth or hundredth of a second. Lines between the instruments show the transition paths that were found in the data, with the two-way transition values indicated. The thickness of the line connecting two instruments is drawn proportional to the value of the two-way transition percentage to facilitate a more rapid visual interpretation of these transition paths. Compare the dwell percentages on the flight director during ILS approaches (figs. 5 and 6) for manual and automatic (coupled) flight modes. Figure 5
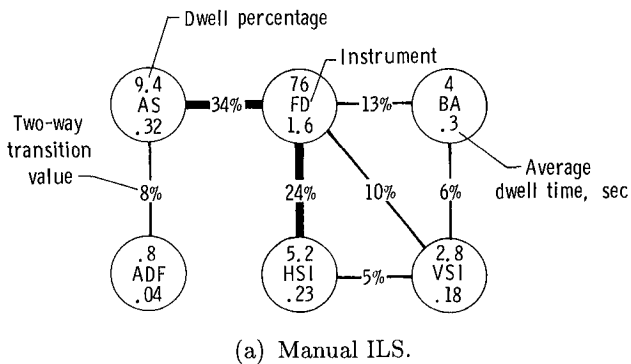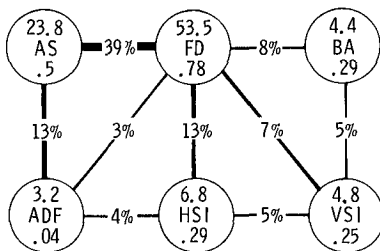
4
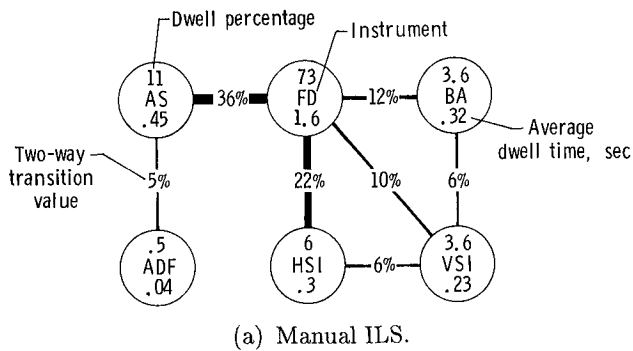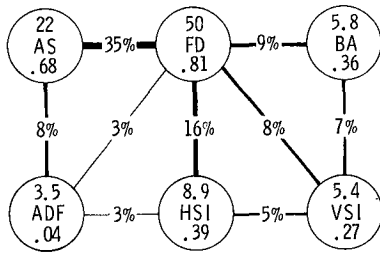
(a) Manual ILS.

(b) Coupled ILS.

Figure 5. Manual and coupled ILS approaches with no atmospheric turbulence. Transition values less than 2 percent were omitted.

(a) Manual ILS.

(b) Coupled ILS.

Figure 6. Manual and coupled ILS approaches with atmospheric turbulence. Transition values less than 2 percent were omitted.

shows data with no turbulence, and figure 6 shows the same data with turbulence. Slightly more of the pilot's attention (dwell percentage on the flight

director) was required with turbulence than with no turbulence.

Appendix B gives a functional description of three computer programs which were developed to analyze pilot scanning data by calculating the transition matrices. These programs are SCAN, SUMMARY, and HISTO.

Statistical tests of scanning-behavior measures.
Differences in independent factors (testing conditions) can be evaluated by using scanning-behavior measures (average dwell time, dwell percentage, and two-way transition probability) as dependent variables. One problem with these statistical tests in the past has been a general lack of consistency in the evaluations from one condition to another. This problem has generally been overcome by the collection of enough data to produce consistent trends. A second problem, the interpretation of changes in the scan measures, has been alleviated by more basic research into scanning behavior and the development of more advanced analysis techniques. A third problem with the average dwell time measure is a lack of sensitivity. For instance, the average dwell time has a large standard deviation, almost equal in magnitude to the average, whether it is measured from one pilot or several. This lack of sensitivity has been overcome by the use of the dwell histogram and the correlation of dwells with pilot activity. (See the section on "Dwell Histograms".)

The computer program summary, described in appendix B, is used to perform standard statistical tests. The output of the summary program consists of four tables, including tables of sums of squares, averages, F ratios of variances, and two-sample t-test values and the associated degrees of freedom. The values in these tables are used to determine whether statistically significant differences exist between conditions.

Dwell Histograms

The answer to the question of why a pilot looks at a display the way he does can be inferred from a histogram of the dwell times on that instrument. A dwell histogram is a graph of either the total number of dwells or the percent of total dwells on an instrument which lasted for the time indicated by the abscissa. Intuitively, the length of the dwell time should be inversely related to the rate of information transfer from the display to the pilot. Longer dwells indicate that more information is being taken in (see the discussion on differences between monitoring and controlling dwells later in this section), that the display is slower in transferring the information (refs. 6

and 7), or that the pilot is staring at the display. At the present time it is left to the judgment and expertise of the experimenter to determine whether the longer dwell time is reflecting slower information transfer, an increased amount of information transfer, or staring.

To demonstrate that the dwell histogram is sensitive to the rate of information transfer in a display, tests in which the format of the directional gyro was altered were conducted in the Langley General Aviation Simulator (ref. 7). One format used a conventional "compass rose"; the other format used a compass rose with a movable "bug" which could be positioned at the desired aircraft heading. It is obvious that the bug is an enhancement to the heading display because with the bug the pilots are able to see the heading error, as indicated by the position of the bug relative to the fixed pointer, instead of having to estimate their heading and mentally compare it with the desired heading of the aircraft. The dwell histograms of the two types of display are presented in figure 7. As expected, the dwell histogram with the bug is further to the left (shorter dwell times) than the dwell histogram without the bug. These results show that the dwell histograms can be useful in evaluating information transfer rate of display formats.
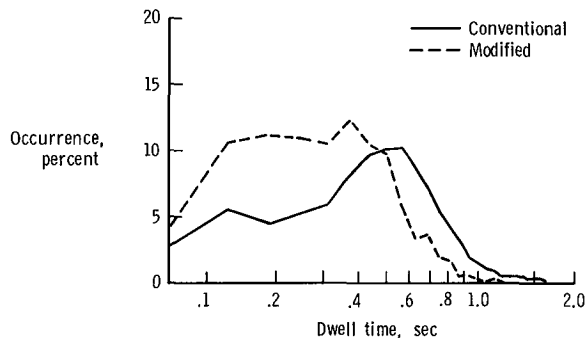

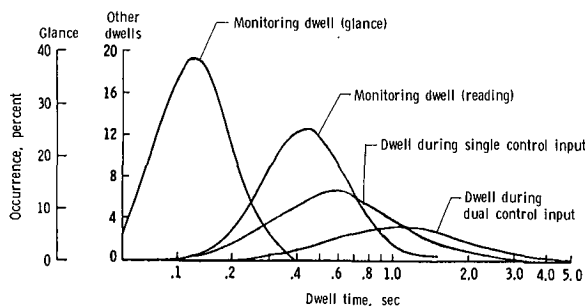Figure 7. Directional gyro-monitoring dwell histogram.

Figure 8. Dwell distributions.

Dwell time has a large standard deviation even if it is measured from just one test subject. One of the first attempts to evaluate the cause of the large variations in dwell times was a correlation of the dwells with certain pilot activities, such as making control inputs, and the examination of the dwell histogram associated with each activity (ref. 8). The resulting dwell histograms show several different distributions. Figure 8 shows four dwell distributions with peaks at 0.1, 0.4, 0.6, and 1.2 sec. When plotted on a logarithmic scale as in this figure, the curves appear symmetrically distributed about their peaks. These curves are all significantly different ($p < 0.01$) when evaluated with the Kolmogorov-Smirnov test (ref. 9). The two distributions with the shortest duration are for monitoring dwells (dwells during which no control input was made), and the two distributions with the longest durations are for control input dwells (dwells during which control inputs were made). It is hypothesized that the monitoring dwell histogram with a peak at 0.1 sec is associated with "subconscious" (nonrecallable) verification of information (i.e., a glance), while the monitoring dwell histogram with a peak at 0.4 sec is associated with "conscious" (recallable) reading of information. The control input dwell histograms are classified according to the number of control inputs made during that dwell. As seen in the figure, dwells longer than 1.0 sec are almost eliminated from the monitoring dwell classification.

Closely associated with the dwell histogram is the fixation histogram. A dwell on an instrument is made up of the series of continuous fixations which remain within the boundary of that instrument. Even though the average dwell time parameter is not a sensitive statistical measure, the fixation time histograms are very consistent from pilot to pilot with similar skill levels and, when separated according to pilot activity such as monitoring or controlling, seem to be insensitive to environmental factors, such as turbulence, or situational factors, such as the maneuver being performed. Turbulence is associated with a reduction in the number of fixations that are linked together to make a dwell rather than with a change in the length of the individual fixations. In one series of tests in a fixed-base simulator in which the effect of turbulence was evaluated, the number of fixations per dwell was reduced, as seen in table I. It appears that the effect of turbulence (or an increase in the frequency content of displayed information) is a reduction in the amount of information gathered only while making control inputs. It could be that the pilot abandons the verification that his input has had the intended effect and instead transitions to another instrument looking for additional information.

6

TABLE I. FLIGHT DIRECTOR FIXATIONS PER DWELL WITH AND WITHOUT TURBULENCE

Type of dwell	Fixations per dwell	
	Turbulence	No turbulence
Monitoring	2.0	2.0
Controlling	4.0	7.0

Figure 9. Pitch control input timing during attitude dwell following an altitude dwell.

Timing of control inputs. Display effects on scanning behavior involve more than just how long a pilot looks at a given display. The format and ease of interpreting a display may have a noticeable effect on the dwell time on the display scanned next, particularly when the pilot is required to mentally assimilate the information gained from the first display. In some cases, dwell time effects may be so subtle that they are not evident in the average dwell time on that instrument. For example, the dwell time on the flight director is already influenced by a variety of factors, as evidenced by its large average and standard deviation. However, effects on the dwell time may be evident in the average duration of the attitude dwell following a look at the display of interest. These carry-over dwell time effects were present in tests reported in reference 10, in which an all-digital altimeter was compared with a conventional counter-drum-pointer altimeter. The average dwell time on the attitude indicator following a dwell on the digital altimeter was increased over the average attitude dwell time after looking at the counter-drum-pointer altimeter. Moreover, when control inputs were made during the attitude dwell after the sequence altitude dwell–attitude dwell, it took longer to make a control input when the altimeter was digital. The two histograms of the timing of the control input are shown in figure 9. Pilots' comments support these oculometric data by revealing that they had to think about altitude more with the digital altimeter than with the counter-drum-pointer altimeter. Consequently, the pilots took longer to assimilate and integrate altitude information with the digital altimeter than with the counter-drum-pointer altimeter.

Statistical tests of histograms. It is quite desirable to determine if two histograms are statistically different from each other because of differences in test conditions. A nonparametric test which can be used for histograms is the Kolmogorov-Smirnov test (ref. 9). This test is used to find the maximum difference between two cumulative distributions (the sum of all histogram levels from the lowest to the current point of interest) and based upon the number of data points in both curves, to determine at
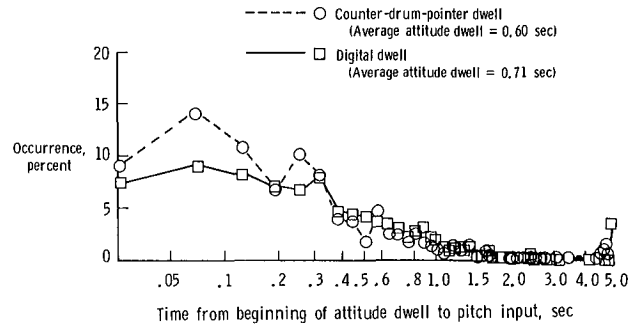
what significance level the two are different. Thus far, this testing procedure has produced results with "face validity," that is, the results of the test are what one would have predicted by looking at the raw histograms.

Measurement of Scanning Randomness

Markov probability transition matrices (refs. 11 and 12) describe the predominant patterns in the scan by means of the relative sizes of transition probabilities, but comparison of two of these matrices for different experimental conditions has proved to be either extremely difficult or impossible. Some researchers (refs. 11 and 12) have used a chi-square test of the transition matrices; however, equivocal results were obtained because some simplifications and manipulations of the data were made which are not supported by any theoretical basis. A goal of scanning-behavior research is to identify a general method for the study of scanning behavior. This method should be independent of the number and arrangement of instruments. The nature of oculometric lookpoint data suggests some methods from information theory (ref. 13) which may have this generality (ref. 14).

The term entropy has been associated with information theory for so long that its usage tends to suggest an attempt to quantify the information content of some system. However, in an even older usage of the term in thermodynamics, entropy is used to describe the amount of disorder (randomness) present in a system. In the present discussion it must be emphasized that the attempt is not to quantify the amount of information which the pilot is acquiring from the displays, but rather to quantify the amount of spatial and/or temporal randomness present in the pilot's scan behavior. This concept coincides with the meaning of entropy in thermodynamics.

The piloting task is such that the pilots' scan is limited to a specified number of instruments (N) at a time. The time history of dwells has a form similar to that of a communication system which can assume

one of N discrete states with a varying duration in each state. The orderliness of such a system is related to the probabilities with which the system occupies its different states. A system that always occupies the same state or always makes the same transitions between states is not random. In the case of instrument scan, these situations would be paralleled by staring or by stereotyped scan patterns. This concept of system order may be stated compactly by using information theory (ref. 13) to generate a mathematical equation for entropy of letter sequences and applying it to instrument sequences scanned. The entropy of the scan becomes

$$H = \sum_{i=1}^{D} H_i = -\sum_{i=1}^{D} p_i \log_2 p_i$$

where

H observed average entropy

p_i probability of transition between two instruments x_{ij} divided by the sum of the off-diagonal terms in the transition matrix

D number of off-diagonal terms in transition matrix $N(N-1)$

N number of instruments

To calculate the entropy, first convert the off-diagonal terms of the transition matrix to percentages by dividing by the sum of the off-diagonal terms. Entropy is the overall sum of the products of each nonzero off-diagonal terms and the base 2 log of the same off-diagonal term of the transition matrix as follows:

$$\begin{aligned} H = - \, (&x_{12} \log_2 x_{12} + x_{13} \log_2 x_{13} \\ &+ x_{21} \log_2 x_{21} + x_{23} \log_2 x_{23} \\ &+ x_{31} \log_2 x_{31} + x_{32} \log_2 x_{32}) \end{aligned}$$

In the case of scanning behavior, entropy has the units of bits per transition and provides a measure of the randomness of the scan behavior. The lower the numerical value of the entropy, the less random (more ordered) is the scan pattern. The maximum possible entropy is constrained by the number of instruments and the number of nonzero off-diagonal terms. The entropy measure uses the probabilities which are present in the Markov transition matrices, but it yields a single, more compact expression of the overall behavior of the probabilities rather than presenting them individually.

While entropy is a measure of the randomness of the scanning behavior, it does not take into account the differences in dwell time for each dwell. Dwell time can be markedly affected during high mental workload situations. To include the effect of time, entropy rate $\dot{H}$ is defined as

$$\dot{H} = \sum_{i=1}^{D} \frac{H_i}{(\text{DT})_i}$$

where

H_i entropy for transition i as given above

$(\text{DT})_i$ average combined dwell time for instruments when transition i occurs

D number of off-diagonal terms in transition matrix, $N(N-1)$

N number of instruments

Entropy rate, like entropy, indicates randomness (in the sense of rate of change in randomness) in the scan pattern. Entropy rate analysis was performed on scanning-behavior data of tests conducted to evaluate two types of vertical speed indicators, VSI's (ref. 6). These tests and others (ref. 14) demonstrated that as the level of mental loading required for a secondary task increases, the entropy rate decreases exponentially (fig. 10, taken from ref. 6). In other words, the scan was more ordered (i.e., less random) with higher mental loading and resulted in a lower value of entropy rate. Therefore, in comparing two systems or displays, the system or display with the lower entropy rate (more ordered scan pattern) would indicate a higher mental workload. The explanation for this effect on entropy rate is that the higher mental loading deprives the pilot of the time needed to make the normal cross checks (i.e., random looks) at other instruments; therefore, he concentrates his scanning on the essential instruments.

The entropy rate for a VSI with a vertical bar graph display format (vertical VSI) and a conventional VSI at different imposed mental workload conditions is plotted in figure 10. The entropy rate, measured in bits per second, of the vertical VSI was greater than that of the conventional VSI. Since increasing the imposed mental workload (task demand) decreases the entropy rate, the curve with the lower entropy rate would indicate the higher workload condition. Therefore, using the conventional VSI imposes the higher workload. An estimate of the magnitude of this difference in workload can be obtained by finding the value of task demand (TD) in the equation for the vertical VSI curve which gives the same entropy rate as the conventional VSI at the zero TD level. This TD value corresponds to flying with the

$$\dot{H} = 1.75 + .5e^{-8\,TD}$$

$$\dot{H} = 1.75 + .5e^{-8\,(TD + .045)}$$

● VERTICAL VSI
○ CONVENTIONAL VSI

ENTROPY RATE, bits/sec

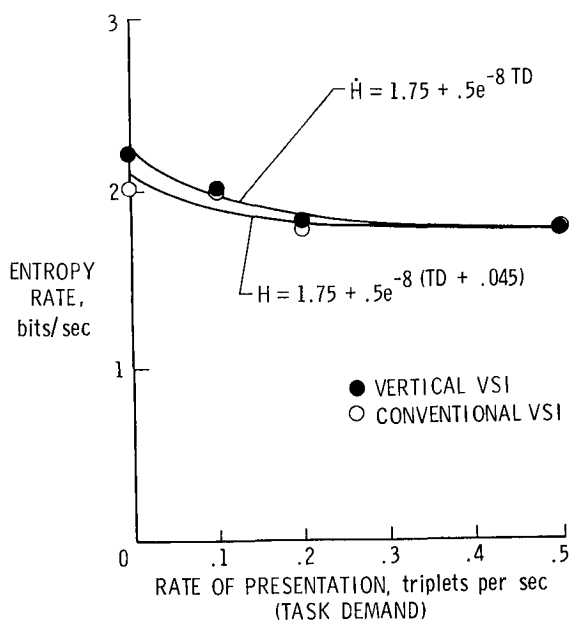RATE OF PRESENTATION, triplets per sec
(TASK DEMAND)

Figure 10. Entropy rate as a function of mental loading.

vertical VSI and performing the mental side task at a level of 0.045 secondary tasks per second for the ILS landing task. Thus, the difference in visual workload is equivalent to performing the mental loading secondary task at a rate of slightly less than 3 per minute.

Other Possible Analysis Methods

The analysis of scanning-behavior data is just in its infancy. Consequently, there are several phenomena which have not yet been investigated in the context of flight simulation. They are discussed in the following sections.

Blinking rate. What affects the timing or rate at which a pilot blinks? Observation of scanning data would seem to indicate that in some circumstances blinking is slowed down when the task is getting more critical (ref. 15). It is not known if this phenomenon is peculiar to a few pilots or if it is applicable to all pilots. It is also not known if there are situations in which the reverse is true, that is, increased blink rate with increased stress.

Pupil diameter. Pupil diameter has been observed to be a function of mental processing of information. However, in scanning-behavior studies thus far, only one study (ref. 16) has noted a consistent trend in pupil diameter (i.e., increase in pupil diameter as the landing approach proceeded). Many factors other than mental stress affect pupil diameter. Examples are ambient light levels and differences in reflectivity

of instruments. (Some are highly absorbent, others are highly reflective.)

Transition path optimization. One method of data analysis which should be pursued is transition path optimization. This would be useful in evaluating graphic displays to determine which symbols to locate adjacent to each other and which ones to place in the periphery (because they are used less frequently).

Application of Scanning-Behavior Analysis Techniques

Scanning behavior and the previously mentioned analysis techniques can be applied to a variety of research issues. The following research issues will be discussed individually: visual workload, information transfer of displays, pilot strategy and role, and pilot training.

Visual Workload

The term workload incorporates all factors which contribute to the level of effort expended by a person to accomplish a task. There is no single measure of total workload, but generally, it is thought that workload can be broken down into at least three categories: physical workload, mental workload, and psychological stress. These categories can be further subdivided into many other factors which affect workload. For example, scanning behavior is primarily related to the mental aspects of workload, that is, the time it takes a pilot to acquire information from displays. For the sake of clarity in this report, this aspect of workload will be called visual workload. One approach is to measure relative amounts of visual workload. Scanning-behavior measures which have been shown to be useful in evaluating visual workload are transition matrix measures (dwell percentage and average dwell time) and entropy rate.

Transition matrix measures. Visual workload measures derived from the transition matrix are dwell percentage and average dwell time. The longer the time spent on an instrument (as measured by either dwell percentage or average dwell time), the greater the visual effort that is expended to obtain information from that particular instrument. This assumes, however, that the same types or amounts of information are being obtained from the instruments. Therefore, it would be inappropriate to compare the dwell percentages and/or average dwell times of an attitude indicator with those of a flight director because more information is displayed in the flight director. However, it would be proper to evaluate

9

the differences in average dwell times or dwell percentages of circular meter movements, vertical meter movements, and digital meter formats for a particular display such as airspeed, directional gyro, or rate of climb indicator.

Entropy rate measures. Another measure which has been shown to be useful in estimating visual workload is entropy rate (a measure of randomness in the total scan pattern). This measure has been used with desktop as well as the more sophisticated simulators and seems to be generally applicable for comparing two different instruments in the instrument cluster while a single task is being performed. It has not worked in simulations of complex tasks in which the instrument evaluated was used primarily during only a small fraction of the entire flight. Properly designed flight tasks are necessary for the use of entropy rate analysis when comparing two instruments.

Entropy rate measures of novice pilots have been shown to be lower than those of fully trained pilots (ref. 17). (Presumably the novice pilots had to work harder than the fully trained pilots.) After training, their entropy rates were the same as those of the fully trained pilots. (See the discussion on training.)

Information Transfer

Histograms can be used to evaluate the rate of information transfer from the display to the pilot. If a pilot accomplishes a task with the same level of performance with a display having a shorter average dwell time, then either the information is transferred from the display more quickly or less information is transferred from the display. The researcher should be guided by experience and pilot comments in deciding which situation is occurring. An obvious example is the difference in dwell percentages with an attitude indicator (50 percent) and a flight director (75 percent) during ILS approaches. Dwell percentages on the flight director are much greater because of the extra displayed information (command bars and raw glide slope and localizer). However, in the case of a digital light-emitting diode (LED) altimeter and a counter-drum-pointer altimeter, the reason for the lower dwell time on the digital altimeter is not quite as apparent. Pilot comments indicate that less information can be obtained from the digital display because of difficulty in perceiving a relative needle position or in obtaining rate clues.

Dwell histograms. The dwell histogram analysis procedure was used to analyze data collected in a six-degree-of-freedom motion-base simulator (ref. 18).

The tests were designed to determine the effects of correct pitch motion, reversed pitch motion, or no motion on pilot scanning behavior in a single-axis tracking task. The results are shown in figure 11 as cumulative fixation histograms. Kolmogorov-Smirnov tests of the three conditions indicated that the two motion conditions were not statistically different from each other ($p < 0.10$) and that both motion conditions (correct and reversed) were statistically different from the no-motion condition ($p < 0.01$). These data, while very interesting, do not by themselves mean that high-fidelity motion is or is not essential. What it does suggest is that there is a cue provided by motion (most likely motion onset cue) that allows the pilot to shorten his dwells over what would be required in a nonmotion simulator to detect motion purely by instrument readouts. It also suggests that in terms of visual workload, any study performed in a fixed-base simulator will predict longer dwell times and slower transition rates than one performed in a motion-based simulator.

Entropy rate. Entropy rate can also be used to evaluate the information transfer rate of displays. (See the discussion in the "Visual Workload" section.) Lower entropy rate indicates higher visual workloads. Estimating the visual workload differences between conditions requires the use of a side task which can be set to various levels of difficulty.

Pilot Strategy and Role

Many times experiments are performed to quantify how pilots normally do some type of activity, for example, where pilots look while landing or where they look on takeoff. The following scanning-behavior analytical techniques have been successfully used to answer these types of questions: time histories, time-locked time histories, and transition matrix measures.

Time histories. If it is known ahead of time that a specific strategy is to be quantified (for instance, how many times a pilot transitions from the window to the instruments on a landing approach), then the researcher may skip the process of actually looking at the time histories and obtain the analyzed data directly from a computer program. However, it is good practice to look at the time histories to determine if some unexpected event may have taken place which relates to the pilot's strategy and would otherwise be left unevaluated.

The time history technique was useful in one investigative study by the authors to identify which instruments pilots use during takeoffs. Particular
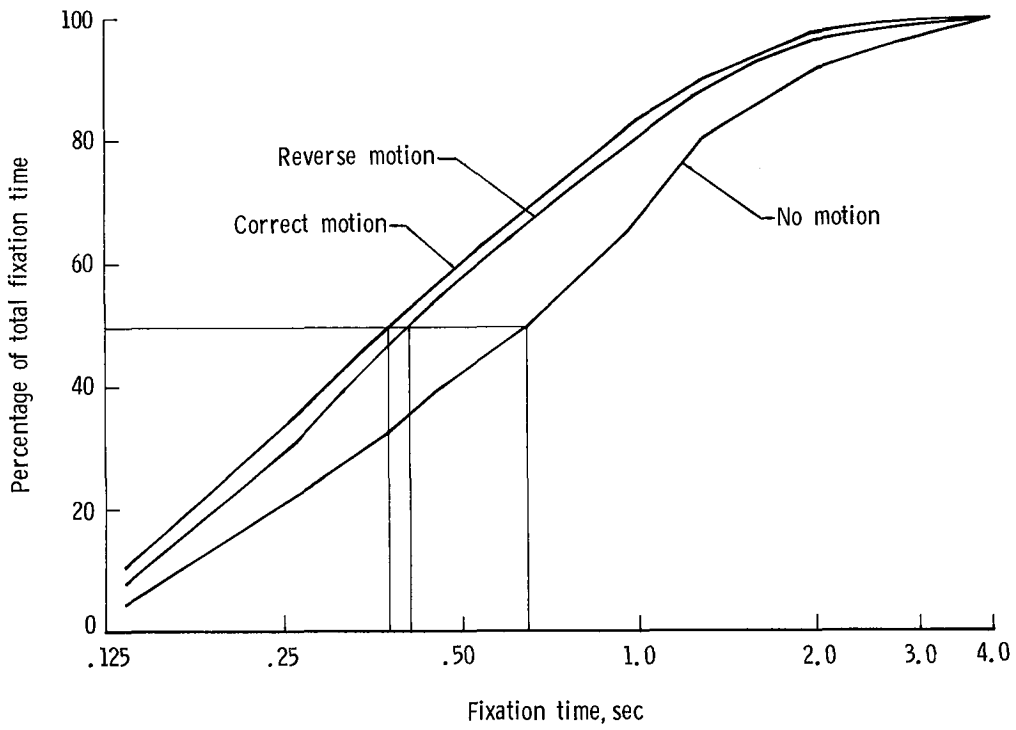
Figure 11. Cumulative plot of fixation time. Experimental data from seven pilots.
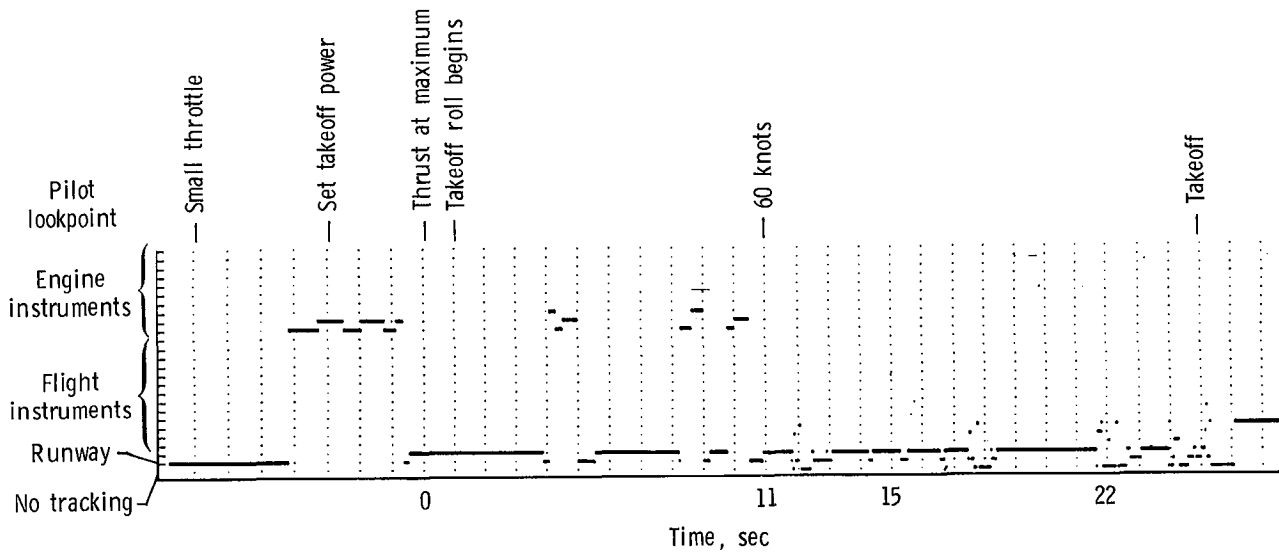

Figure 12. Pilot scan during takeoff.

emphasis was placed on scan patterns of engine instruments during takeoff. For the purposes of these tests, the lookpoint data (instrument being monitored) were plotted as time histories, and the pattern of engine instrument usage was evaluated by visual inspection. Figure 12 shows such a time history. The 10 instruments at the top of the ordinate are the engine instruments in question. In the general pattern, the pilot looked at the engine instrument cluster three to four times during a takeoff. During the first look, he verified that the instruments were responding smoothly and normally to a small throttle increase. The second look occurred when takeoff thrust was applied. This second look sometimes included only the instrument monitoring engine pressure ratio (EPR) because the pilot was aiming for a specific EPR reading to take off. The third look was made just before the airplane reached 60 knots. With this look, the pilot verified that takeoff power had been set to the proper EPR value. There may or may not have been a look at the instrument monitoring engine speed. Finally, there may or may not have been one more look at the engine instruments before takeoff rotation.

Time-locked time histories. A second analysis tool that has been useful is the time-locked time history. As seen in figure 4, there seems to be a definite strategy on what to look at after the secondary task is over: first a blink (short out-of-track), then a look at the attitude indicator, and then a look at the directional gyro. Pilot differences in scanning strategy could also be revealed with this analysis technique by comparing the pilots' patterns of instrument usage.

Transition matrix measures. A third analysis tool that has been useful is the transition matrix. Dwell percentages could show increased or decreased use of a particular instrument. Transition percentages could show changes or additions to normal or particular patterns used to scan the instruments. Figure 13, taken from reference 19, shows the dwell times, dwell percentages, and transition percentages of two types of landing approaches flown with electronic attitude and horizontal situation indicators. One approach was a straight-in landing approach, and the other was a curved, descending approach. Not only are there significant differences in the transition percentages between instruments, but there is also a new transition path with the curved approach between the electronic horizontal situation indicator and the airspeed indicator. This new transition path indicates that a new arrangement of the panel with a side-by-side arrangement of the electronic displays might

not be a good design because of the increased physical separation between the airspeed display and the electronic horizontal situation indicator.

Pilot Training

In some simulator studies, situations arose in which the experimenter felt the pilot was not using the instruments properly. When questioned about their use of the instruments and shown the video playback, the pilots usually agreed that an improvement could be made by modifying their scanning behavior. In another study (ref. 17), both trainees and instructors were able to apply scanning-behavior data beneficially in a formal pilot training program.

Video playback. A pilot training program was conducted for LaRC by Old Dominion University researchers at Piedmont Aviation. Piedmont instructors and transition trainees were used in the program (refs. 20, 21, and 22). The results indicated that qualitative data obtained from a video tape telling pilots how they scan had some value and that scanning-behavior feedback from the instructors or from the trainees viewing their own scanning behavior can be a very useful tool for pilot training. The degree of usefulness of the scanning-behavior feedback is a function of the trainee's needs in establishing a good mental picture of the task to be accomplished. The instructor pilots found the availability of real-time scanning data useful during the training session in which flight technical errors were encountered. The transition trainee pilots found that studying the video playback was helpful in correcting errors and in developing general piloting skills.

Dwell histogram. One way a pilot learns is by watching the instruments to see their responses to his inputs. As he learns what to expect from the instruments, he no longer has to look at them as long. This learning process should show up in the average dwell time and in either the dwell histogram or the fixation histogram as shorter values for the peaks and fewer long dwells.

Entropy rate. Preliminary analysis indicates that the entropy rates of trainees start very low (quite orderly) but approach the level of instructor pilots at the end of the training session. In other words, the trainees' scan patterns are very structured at first because of unfamiliarity with the task, but as they learn the task, they rely more on reflexes or a "mental picture" of the way the aircraft will function. Consequently, they do not have to deliberately think about each item or step. Their scan patterns begin
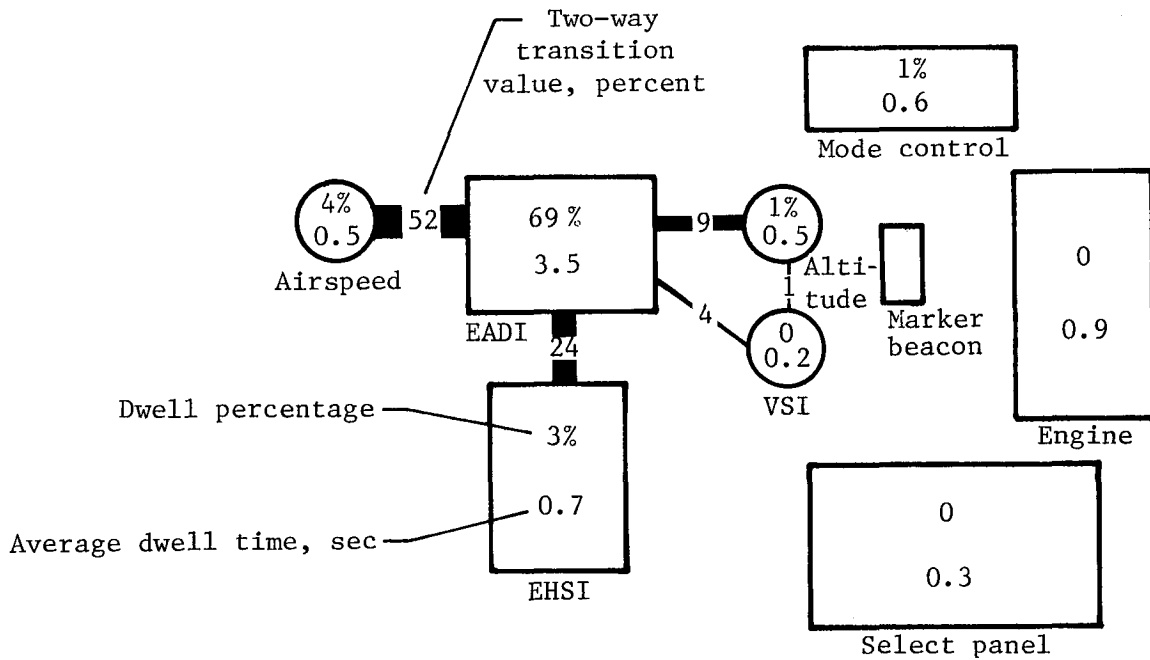
(a) Straight-in approach.
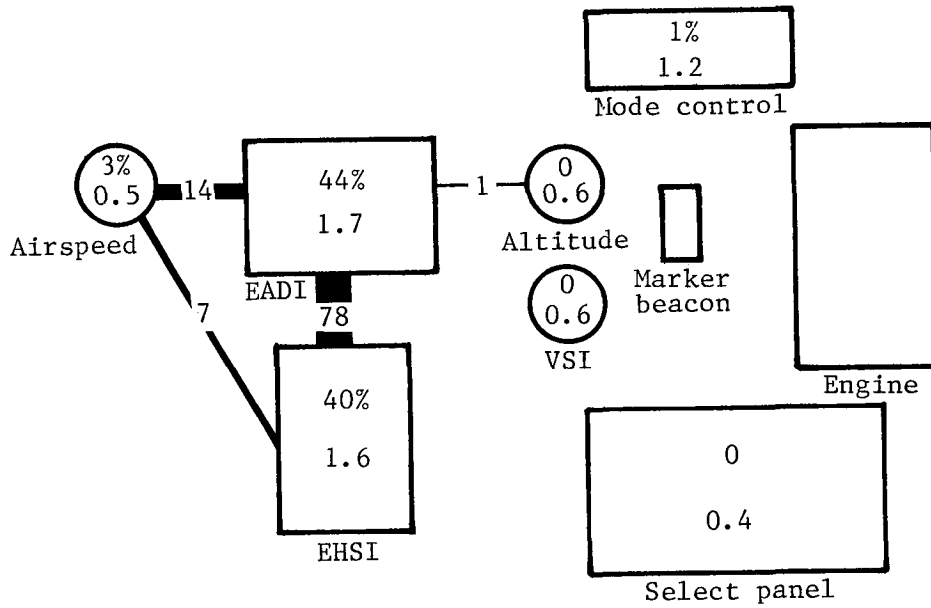
(b) Curved approach.

Figure 13. Dwell times, dwell percentages, and transition percentages for curved and straight-in approaches. Absence of data indicates absence of pilot scan.

to "loosen up", that is, they are able to observe secondary information (more random scanning) and still fly the airplane satisfactorily. This analysis demonstrates that there is a significant amount of visual workload involved in the learning process and that the subjective impression of a higher workload for a novice is based upon the fact that the learning process affects the workload.

Concluding Remarks

This report documents the state of the art of oculometric data analysis techniques and their applications in certain research areas such as pilot workload, transfer of information from displays to pilots, strategy and role of pilots, and pilot training. These techniques include real-time viewing of the pilot's scanning behavior, average dwell times, dwell percentages, instrument transition paths, dwell histograms, and entropy rate measures. Workload estimates are obtained from dwell percentages and entropy rate measures. Information transfer evaluations are performed primarily with dwell times, dwell histograms, and entropy rates. Pilot strategy and role are determined by using scan time histories, time-locked time histories, and transition matrix data. Pilot training evaluation uses real-time scanning data and entropy rate measures. Overviews of the experimental setup, data analysis techniques, and software are presented. A glossary of terms frequently used in pilot scanning behavior and a bibliography of reports on related research sponsored by NASA Langley Research Center are also included.

NASA Langley Research Center
Hampton, VA 23665-5225
March 28, 1986

References

1. Jones, Richard E.; Milton, John L.; and Fitts, Paul M.: *Eye Fixations of Aircraft Pilots, I. A Review of Prior Eye-Movement Studies and a Description of a Technique for Recording the Frequency, Duration, and Sequences of Eye Fixations During Instrument Flight.* USAF Tech. Rep. No. 5837, U.S. Air Force, Sept. 1949.

2. McCormick, Ernest J.: *Human Factors in Engineering and Design,* Fourth ed. McGraw-Hill Book Co., c.1976.

3. Airworthiness Standards: Transport Category Airplanes. FAR Pt. 25, FAA, June 1974.

4. Bourne, J. R.: *Laboratory Minicomputing.* Academic Press, 1981.

5. Spady, Amos A., Jr.: *Airline Pilot Scan Patterns During Simulated ILS Approaches.* NASA TP-1250, 1976.

6. Harris, Randall L., Sr.; Tole, John R.; Ephrath, Arye R.; and Stephens, A. Thomas: How a New Instrument Affects Pilots' Mental Workload. *Proceedings of the Human Factors Society 26th Annual Meeting,* Richard E. Edwards, ed., 1982, pp. 1010–1013.

7. Spady, Amos A., Jr.; and Harris, Randall L., Sr.: Summary of NASA Langley's Pilot Scan Behavior Research. *Second Aerospace Behavioral Engineering Technology Conference Proceedings,* P-132, Soc. Automot. Eng., Inc., 1983, pp. 91–99. (Available as SAE Paper 831424.)

8. Harris, Randall L., Sr.; and Christhilf, David M.: What Do Pilots See in Displays? *Proceedings of the Human Factors Society, 24th Annual Meeting, Human Factors: Science for Working and Living,* George E. Corrick, Eric C. Haseltine, and Robert T. Durst, Jr., eds., 1980, pp. 22–26.

9. Siegel, Sidney: *Nonparametric Statistics for the Behavioral Sciences.* McGraw-Hill Book Co., Inc., 1956.

10. Harris, Randall L., Sr.; and Glover, Bobby J.: Effects of Digital Altimetry on Pilot Workload. Paper presented at the 1984 SAE Aerospace Congress & Exposition (Long Beach, Calif.), Oct. 15–18, 1984.

11. Stark, Lawrence; and Ellis, Stephen R.: Scanpaths Revisited: Cognitive Models Direct Active Looking. *Eye Movements: Cognition and Visual Perception,* Dennis F. Fisher, Richard A. Monty, and John W. Senders, eds., Lawrence Erlbaum Assoc. Publ., 1981.

12. Krebs, Marjorie J.; and Wingert, James W.: *Use of the Oculometer in Pilot Workload Measurement.* NASA CR-144951, 1976.

13. Shannon, Claude E.; and Weaver, Warren: *The Mathematical Theory of Communication.* University of Illinois Press: Urbanna, 1949.

14. Tole, J. R.; Stephens, A. T.; Vivaudou, M.; Ephrath, A.; and Young, L. R.: *Visual Scanning Behavior and Pilot Workload.* NASA CR-3717, 1983.

15. Stern, John A.; Walrath, Larry C.; and Goldstein, Robert: The Endogenous Eyeblink., *Psychophysiology,* vol. 21, no. 1, Jan. 1984, pp. 22–33.

16. Harris, Randall L., Sr.; and Mixon, Randolph W.: Advanced Transport Operation Effects on Pilot Scan Patterns. *Proceedings of the Human Factors Society 23rd Annual Meeting,* Carolyn K. Bensel, ed., 1979, pp. 347–351.

17. Jones, Dennis H.: *An Error-Dependent Model of Instrument-Scanning Behavior in Commercial Airline Pilots.* NASA CR-3908, 1985.

18. Comstock, James R., Jr.: *Oculometric Indices of Simulator and Aircraft Motion.* NASA CR-3801, 1984.

19. Harris, Randall L., Sr.; and Mixon, Randolph W.: *Effects of Curved Approach Paths and Advanced Displays on Pilot Scan Patterns.* NASA TP-1846, 1981.

20. Spady, Amos A., Jr.; Jones, Dennis H.; Coates, Glynn D.; and Kirby, Raymond H.: The Effectiveness of Using Real-Time Eye Scanning Information for Pilot Training. *Proceedings of the Human Factors Society 26th Annual Meeting,* Richard E. Edwards, ed., 1982, pp. 1014–1017.

21. Jones, Dennis H.; Coates, Glynn D.; and Kirby, Raymond H.: *The Effectiveness of an Oculometer Training Tape on Pilot and Copilot Trainees in a Commercial Flight Training Program.* NASA CR-3666, 1983.

22. Jones, Dennis H.; Coates, Glynn D.; and Kirby, Raymond H.: *The Effectiveness of Incorporating a Real-Time Oculometer System in a Commercial Flight Training Program.* NASA CR-3667, 1983.

Appendix A

Overview of Oculometer System

Daniel W. Burdette
PRC Kentron, Inc.
Hampton, Virginia

Development of Oculometer

The oculometer system used in simulation and laboratory studies at LaRC was a highly modified version of the Honeywell Mark 3A remote oculometer (refs. A1–A3), which allows head movements by a subject of up to 1 ft^3. Basically, the system operates by projecting a beam of collimated infrared light at one of the subject's eyes (fig. A1). Two reflections from the eye are returned to a video camera. The first is a broad (4- to 8-mm) reflection of the retina, bounded by the pupil, like a cat's eye reflecting from the headlight of a car; the second is an intense pinpoint reflection from the surface of the cornea. From the video signal of the eye's reflections, the computer determines the center of each reflection. Based upon the relative positions of the reflections, the computer, calculates the pilot's foveal lookpoint on the instrument panel. A video tape of the instrument panel and the pilot's superimposed lookpoint is saved as a permanent record of the test. The lookpoint coordinates and pupil diameter are recorded for subsequent computer analysis. Recordings of the aircraft state variables, pilot control inputs, and other measures of interest can be recorded at the same intervals for use in correlating pilot lookpoints with flight conditions and other factors.

Hardware modifications. Several hardware modifications were made to the original Honeywell system to increase the utility of the oculometer system. The primary modification was made to the electro-optic (EO) head. Figure A2 shows the EO head as received from Honeywell. The TV camera inside the EO head was replaced by a smaller one, and internal wasted space was eliminated. The resulting EO head (fig. A3) was about one-third the size of the original head. The next change was the addition of analog output channels so that the oculometer could output not only the lookpoint coordinates but also a voltage proportional to the instrument being observed at by the subject. This feature allowed easier recording of data by external microcomputers, such as the one in figure A4. The infrared light source and collimation scheme were modified next so that a 15-W bulb could replace the 150-W projection bulb. This modification eliminated the need for a large heat sink and cooling fan and further reduced the size of the EO head to its current size of about one-fourth the original size (fig. A5). This size reduction was enough to allow the EO head to be placed behind many simulator instrument panels (fig. A6). The last hardware modification was the addition of a single-chip microprocessor to process eye data in parallel with the oculometer computer. Its only function was to position the two tracking mirrors to keep the eye's reflections in the center of the TV image. The effective tracking speed of the mirrors increased by over a factor of two, and the tracking time of the oculometer on a typical run improved from about 75 to 95 percent. The remaining out-of-track time is caused by subject eye blinks and a very rare loss of track due to excessive head movement.

Software. A number of oculometer software modifications were made to the original Honeywell oculometer software to make it more user friendly and versatile. Software was added that would automatically adjust calibration coefficients based upon lookpoints collected while the object looked at several (up to 28) calibration points. Improved eye center determination routines were developed that would minimize the effects of upper and lower eyelid distortions of the returned pupil reflection. Provisions were also made for instrument panels of complex geometries, such as those with flat panels at an angle to the main panel or panels located

in front of or behind the main panel. Finally, better terminal communication routines were written to allow the operator to interact in real time with the oculometer computer instead of having to stop the computer from processing eye data and go into the communication mode exclusively.

The volume of data generated during a test makes computer processing a necessity. Initially, no software for data recording and reduction was available for scanning behavior. Software programs have been developed that will process the data into standardized formats. (Appendix B describes three of these programs in more detail.) Inputs to the program are instrument boundaries and conditional flags to direct the type of processing and output generation. The output data from these programs can later be summarized and statistically tested. Every attempt has been made to standardize the data recording procedure to minimize the software changes required from test to test. However, every study has required software changes because of unique test goals, designs, simulator/aircraft configurations, and other constraints.

Outline of Hardware and Procedures for Current Oculometer System

I. Functional description of hardware subsystems and components
   A. EO head
      1. A beam of parallel light rays (wavelength of 800 to 900 nm) is produced by several internal components: a tungsten filament source (6 V/15 W), an IR filter to remove most visible light, a heat filter to prevent unwanted far-infrared energy, two collimating lenses, and a beam splitter.
      2. The moving mirror assembly contains separate azimuth and elevation mirrors to direct the IR beam toward the eye of a test subject. The servo system can be manually controlled, operator assisted through the use of a computer-interfaced joystick, or driven solely by either the Nova computer or a separate and dedicated microprocessor circuit.
      3. Image collection optics, including the positive lens, the servo-positioned negative lens, and folding mirrors combine to focus the eye image onto the surface of a silicon matrix vidicon tube. The motorized positioning system for the negative lens is mechanically coupled to a multiturn potentiometer which provides focus distance information necessary for lookpoint calculations.
      4. A Dage-MTI television camera (black-and-white) model SC-21 with a horizontal resolution of 450 TV lines and a vertical resolution of 375 lines is used. The camera contains a General Electric type Z7996A silicon matrix vidicon tube (1 in.), which efficiently responds to the near-infrared wavelengths present in the focused eye image. The television picture is further enhanced through the use of nonstandard adjustments to the camera control unit, which produce maximum contrast between the pupil and cornea reflections while reducing nonessential details of the eye and skin to the video black reference level. The resulting eye image forms the basis for the entire oculometer system, and it is from this one analog signal that all subsequent data are derived.
   B. Oculometer control unit
      The oculometer control unit (LaRC design) provides manually variable alternating-current (AC) voltage to control the intensity of the tungsten filament light source, control voltages for azimuth and elevation mirrors used to follow the eye, and adjustment voltages to the scan converter for matching the scene camera video to the ideal point and lookpoint output. (See section III.A.5.)

C. Closed-circuit television
   1. Video cameras and monitors
      a. The EO head camera operates in conjunction with a rack-mounted control unit.
      b. The cockpit scene camera (in sync with the EO camera) is used to provide a picture of the cockpit instrument panel upon which lookpoints and ideal points can be superimposed. This video presentation transforms the rather abstract analog voltage outputs from the oculometer into a real-world and real-time picture of eye scanning behavior.
      c. The head tracker camera gives the operator a view of the subject's face for coarse positioning of the IR beam when using either the manual control knobs or the joystick.
      d. Triple 5-in. black-and-white monitors are used for simultaneous viewing of all three video signals.
   2. Video signal processing devices
      a. A combination video data insertion generator/sync stripper provides horizontal and vertical drive signals to the interrupt-driven oculometer program, as well as to the scene camera. In addition, a small insert of the eyeball portion of the EO video is placed into the scene video for tape recording and subsequent diagnostic review, if necessary.
      b. The sync delay unit works in conjunction with the above device to position the eye image insert.
      c. The video tape recorder is a 1/2 in. reel-to-reel model.
      d. A video timer superimposes the date and time on the combined video signals for later reference.
      e. The scan converter is a type of storage oscilloscope which displays the analog outputs from the Nova computer in graphic form and superimposes the lookpoint dot or ideal point dots onto the combined scene television picture.
      f. The television waveform monitor is an oscilloscope specifically designed for viewing composite television signals.
D. Computer system
   1. The Nova 800 computer system accepts video data in analog form, digitally calculates a lookpoint, and provides analog voltages representing x and y coordinates of the lookpoint, as well as pupil diameter data, azimuth and elevation mirror commands, and error codes to help diagnose out-of-track conditions.
   2. The Intel 8751 signal-chip microcontroller, working in conjunction with the Nova computer and assembled as a plug-in board for the Nova card cage, provides improved real-time tracking of a moving eyeball and relieves the main computer of a time-consuming task.
   3. The computer terminal allows operator interaction with the program and provides hard copy through its thermal printer.
II. Setup procedures
   A. Preliminary site survey
      1. Outside cockpit
         Choose a location for the system rack, taking into account AC power requirements (110 V/15 A) and cable routing between the rack and the cockpit. Dedicated cables exist at LaRC between some flight simulators and a central oculometer laboratory. A single AC power line should be used for all oculometer equipment to avoid electrical noise. In some simulators it has been necessary to magnetically shield and electrically insulate components from interference within the cockpit.

2. Inside cockpit
   a. Decide on the test subject's visual area of interest within the total instrument panel (typically limited to approximately 40 in. horizontally by 20 in. vertically).
   b. Choose an EO head location from several possibilities. The following factors should be considered:
      (1) The mirror box assembly must fit into the simulator with minimum disruption of the normal instrument panel configuration.
      (2) Optical paths should be as short as possible and should avoid the chance of IR beam obstruction during any phase of the flight simulation.
      (3) The mirror box must be near the bottom of the area of interest to avoid eyelid obstruction of the pupil. Any glances below the level of the mirror box will inevitably cause the subject's upper lid to droop.
      (4) The blind spot of the eye should be avoided, since the pupil return is greatly diminished. For example, if the left eye must be avoided in a particular cockpit because of control yoke blockage of the light beam, avoid placing the mirror box such that the IR beam will strike the blind spot in the subject's right eye each time an important instrument is viewed.
      (5) The face of the mirror box should be coincident with the fixation plane to minimize large geometrical compensations in the program.
   c. Choose a location for the scene camera to provide an undistorted and unobstructed view of the area of interest on the instrument panel.
   d. Choose a location for the head tracker camera that gives a clear view of the subject's face without causing a great deal of visual distraction.
   e. Plan to locate the mirror amplifier within 10 ft of the EO head to minimize cable losses. In motion-based simulators all hardware must be mechanically secure.
B. EO head configuration and calibration
   1. Orient the vidicon mechanically and electrically such that with the camera pedestal control turned up, a focused image (such as that of a ruler) appears on the monitor as correct (i.e., right side up and nonreversed horizontally). Minimize optical reflections within the EO head by coating bright surfaces with optically flat black paint.
   2. While observing the composite video output on the TV waveform monitor, decrease the camera pedestal control until a clear image of an artificial eye is produced with the pupil reflection at approximately 0.5 V and the cornea reflection at 1.0 V. Also insure that the image is free of extraneous video information due to optical reflections or electrical noise, since such artifacts can cause the moving-mirror servo system to track false targets. Other potentially damaging effects include erroneous data output and complete loss of track during system operation.
   3. Measure the image collection optics and enter scaled machine values of the distances and focal lengths into the program by using the multiplication factors and computer symbols listed in table AI.
   4. Center the light source for maximum pupil return of an artificial eye as the image is moved across the center of the vidicon by manually controlling the mirrors. The beam splitter should be positioned such that the collimated light beam and the television camera share a common optical axis.
   5. Measure the angles at the zero position of the azimuth and elevation mirrors relative to the mirror box. Any variation from the nominal 45° for each must be entered into the program in the form of direction cosines or mirror box pitch-up. Notice that a mirror position offset of 1° results in a deflection of 2° of the IR beam. Of course, the mirrors must be able to rotate sufficiently to track an eye in any location within the cubic foot of space. Section II.C contains more information on the oculometer program geometry.

6. Measure the IR irradiance of the eyespace (30 in. from the face of the mirror box). Vary the intensity, and note the voltage when irradiance reaches 1.67 mW/cm² (10.8 mW/in²), the upper limit allowable for use at LaRC. A more detailed discussion of safety procedures is contained in section III.D of this outline.

C. Geometry

1. With the EO head installed in the cockpit, establish a reference point on the fixation plane. Express any offsets between this point and the origin of the oculometer axis system as X0, Y0, and Z0 in the program. See table AII(a) for the equations used to calculate the offsets. The origin of the oculometer axis system is the point at which the center of the IR beam intersects the face of the mirror box when the mirrors are at their null position (0,0 volts). A convenient way to choose the fixation plane reference point is to look directly into the IR beam with the mirrors at their null position. Then by extending this line of sight through the mirror box, the reference point can be marked on the instrument panel for use in later measurements. Since this point lies within the oculometer Z-axis, the horizontal and vertical offsets are equal to zero (X0 = 0, Y0 = 0). The symbol Z0 equals the distance in inches between the mirror box face and the fixation plane reference point multiplied by 256. When the fixation plane lies behind the mirror box, Z0 is negative.

2. Calculate and enter the constants representing mirror box pitch-up and fixation plane direction cosines. (See tables AII(b) and AII(c).) First, measure the angle between the oculometer Z-axis (a line directly along the IR beam with the mirrors at their null position) and the fixation plane Z-axis (a line perpendicular to the instrument panel originating at the reference point). Then use this angle to determine which of the following three calculation methods is appropriate:

   a. The angle between the two axis systems is zero. In this ideal installation, the mirrors are mounted in the mirror box at their nominal position of 45°, and the IR beam that emerges is perpendicular to both the mirror box and the instrument panel. There is no mirror box pitch-up (D1 = 0, D2 = 16 384), and all direction cosine constants have the following nominal values:

Q1 = 1024	Q2 = 0	L3 = 0
M1 = 0	M2 = 1024	M3 = 0
N1 = 0	N2 = 0	N3 = 1024

   b. The angle has a vertical offset resulting from a pitch-up of the mirror box relative to the instrument panel. All direction cosine constants remain nominal as in the previous example.

   c. The angle has both vertical and horizontal offsets. Once the pitch and yaw components of this angle have been determined, the values for the direction cosine constants can be calculated by using the equations given in table AII(c). For simplicity, it is best to assume in this case that the pitch-up angle of the mirror box is equal to zero (D1 = 0, D2 = 16 348). In all direction cosine calculations, the roll angle can be reduced to zero by properly rotating the EO camera vidicon as described in Section II.B.1.

3. Choose a digital-to-analog conversion scale factor such that an output of ±5 V from each lookpoint channel is sufficient to cover the visual area of interest (table AII(d)). For example, a scale factor of 0.25 V/in. allows coverage of an instrument panel approximately 40 in. by 40 in. (SCFX2 = 1638, SCFY2 = 1638.)

4. Specify the desired output voltages when the subject looks at the infrared light source by calculating and entering machine values for DDX and DDY according to the equations shown in table AII(e). The purpose of DDX and DDY is to allow the operator to set the voltage output when the subject looks at the EO port. Since the

EO port is not usually located at the center of the instrument panel, these values also define the location of the point on the instrument panel which corresponds to a system output of zero volts in both the x and y channels. Careful choice of DDX and DDY can also help to avoid exceeding the analog output limitations of ± 5 V when the subject looks at instruments located at relatively large distances from the center.

5. Specify CALX and CALY coordinates such that approximately three fourths of the total visual angle is covered in each direction from the instrument panel reference point (table AII(f)).

6. Establish the fixation plane ideal points to be used in both the start-up and eye calibration phases of system operation. In a typical flight simulator, it will be necessary to measure and note the horizontal and vertical distances between the center of each instrument and the fixation plane reference point. Enter scaled values of these measurements as appropriate $(TX)_n$ and $(TY)_n$ constants for the various instruments. (See Table AII(g).)

7. Choose a home base point, such as the center of the attitude indicator (flight director), and set XCNTR and YCNTR for quick adjustment of the lookpoint during experimental sessions. (See table AII(h).) Switch no. 13 on the front panel of the Nova computer can force the lookpoint to this position at any time. When used judiciously by a skilled oculometer operator, this feature can greatly improve the accuracy of the data output.

8. Fine tune the description of EO head optics by adjusting computer constants FA0 and RS0 according to the successive approximation formula provided in volume 1 of the operating manual for the oculometer (ref. A3). Adjust constant L9 so that a constant pupil diameter output is obtained when an artificial eye is focused at various points within the cubic foot of eye space. After L9 has been adjusted, print out the values MAG and CMAG. Change CMAG according to the equations shown in table AI. Use the printed value of CMAG as $CMAG_{OLD}$.

9. Verify the accuracy of these steps by checking E3 for several eye focus distances. The symbol E3 represents the distance from the fixation plane to the subject's eye. Also check for proper lookpoint output for various horizontal and vertical rotations and translations of both an artificial and a human eye.

III. Operating procedures
  A. Start-up
    1. Turn on the power to the main equipment rack, the mirror amplifier, and the scene- and head-tracking cameras.

    2. Set switch no. 10 on the front panel of the Nova computer up (all others down) and start the oculometer program by activating the "stop," "reset," and "start" control switches. Three calibration points should be visible on the scan converter. (Increase the intensity if necessary.)

    3. Set ZOFFX and ZOFFY to 0 by typing the name of each constant followed by a slash (/) on the terminal keyboard. After each stored value is printed by the program, simply type in the new value. Numerical values are always considered to be octal unless followed by a decimal point.

    4. Set switches no. 6 and 7 up to generate ideal points on the scan converter and the scene monitor. Use the storage mode of the scan converter to freeze these dots on the scene monitor. Whenever adjustments are made, the previous positions should be erased.

    5. Align the ideal points with their corresponding locations on the instrument panel as represented on the scene monitor. Distortions can be reduced or eliminated by adjusting the appropriate potentiometers for vertical or horizontal gain, bias, and cross talk. The video systems and oculometer program are now internally calibrated

such that a given lookpoint output from the computer will appear at the proper location on the video image from the cockpit scene camera. It should be noted that these corrections do not alter the output of the oculometer computer, but they simply aid in presenting the data in a form which improves system operation, calibration, and interpretation.

6. Verify all data links between the oculometer system and the data collection computers. System output data can be artificially manipulated by a combination of software and hardware adjustments.

7. Set the date and time on the video timer.

B. Eye calibration

1. Enable the servo-driven mirror system and set switch no. 6 up on the Nova front panel to begin tracking the chosen eye of the test subject. It will be necessary to adjust the IR beam intensity for a good video signal. Verbally direct the subject's view to the instrument panel home base, usually located at the center of the flight director. Force the lookpoint output to this position by flipping switch no. 13 up and down. Voltage offsets ZOFFX and ZOFFY are thus added to the oculometer digital-to-analog outputs. The scene monitor should now display a small dot in the center of the flight director. Decrease the intensity of the scan converter until the dot disappears when the eye is out of track (e.g., during each eye blink).

2. As the operator verbally directs the subject's gaze to various instruments on the panel, the linearization coefficients (see table AIII) can be adjusted to correct for any distortions in the lookpoint output due to the eye itself. Unpredictable results can occur if this procedure is attempted before the internal calibrations are completed. (See section III.A.5 of this outline.)

3. Observe the electrical representation of the video signals from the pupil and cornea as seen on the waveform monitor while the subject scans the instrument panel. Large changes in amplitude for various look angles indicate that the reflectivity of the retina is inconsistent and suggest that an automatic intensity controller be used for a more steady IR return.

4. Adjust the servo-driven mirror control system for push-button return to a nominal eye position by reading values of MCX and MCY at an appropriate moment and then inserting these values into computer memory locations MCXHL and MCYHL, respectively. The constants MCX and MCY represent actual mirror command voltages sent to the yaw and pitch mirrors, respectively.

5. Print the values of all linearization constants as well as both ZOFFX and ZOFFY for later reference. Saving a hard copy of this information for each test subject simplifies future calibrations and improves the efficiency of system operation during test sessions.

C. Data collection

1. Prior to the start of the simulation scenario, set switch no. 6 up, enable the mirror servos, and adjust the IR level to begin tracking the test subject's eye, which must be the same eye as that used for calibration.

2. Recheck the offsets by requesting a brief, but steady, glance at the home base of the instrument panel. Corrections may be made either by typing the previously listed values of ZOFFX and ZOFFY or simply by using switch no. 13 at the proper time.

3. Start the video tape recorder at the beginning of each period of data collection.

4. At the conclusion of each run, stop the video recorder, decrease the IR intensity, and set switch no. 10 up to place the computer in a pause mode.

5. At the end of the daily session, set switch no. 10 up and stop program execution with the "stop" switch. Turn off the main rack circuit breaker and all other equipment. Record essential details of the session in the oculometer log.

D. Safety

Although the IR level required for good oculometer operation is quite low, LaRC maintains certain standards for eye safety. The maximum irradiance measured at an eyespace 30 in. from the face of the mirror box should not exceed 1.67 mW/cm^2 (10.8 mW/in^2). This measurement must be performed at least once for each 25 hours of oculometer operation and entered into a permanent log. The log entries, which are initialed by the system operator, include such relevant information as the location of the installation, the name of the test subject, and the total daily time in use. As a further precaution, baseline and semiannual eye examinations are required for each test subject.

References

A1. Merchant, J.; and Morrisette, R.: Remote Measurement of Eye Direction Allowing Subject Motion Over One Cubic Foot of Space. *IEEE Trans. Biomed. Eng.*, vol. BME-21, no. 4, July 1974, pp. 309–317.

A2. Spady, Amos A., Jr.: *Airline Pilot Scan Patterns During Simulated ILS Approaches.* NASA TP-1250, 1976.

A3. *The Honeywell Mark 3A Remote Oculometer Operating and Maintenance Manual,* Volumes 1, 2, and 3. Honeywell Radiation Center, June 1973.

Symbols and Abbreviations

ASCII	American Standard Code for Information Interchange
CALX, CALY	distances from reference point to arbitrary horizontal and vertical calibration points on the fixation plane
CMAG	constant used to adjust the value of MAG
DDX, DDY	offsets used in specifying a zero-volt output from both x and y data channels
EO	electro-optic
IR	infrared
MAG	magnification of oculometer image collection optics
ZOFFX, ZOFFY	computer constants representing voltage offsets used to force the oculometer system output to the chosen home base point on the instrument panel

TABLE AI. CONVERSION OF EO HEAD DIMENSIONS TO MACHINE VALUES

(a) Definition of parameters

Parameter[a]	Multiplication factor	Program symbol
Focal length of positive lens	1024	F1
Focal length of negative lens	1024	F2
Distance between camera face and positive lens	1024	L1
Distance between negative lens and camera face	1024	FA0
Distance between yaw mirror and positive lens	256	RS1
Distance between yaw mirror and pitch mirror	256	RS2
Distance between pitch mirror and electro-optic port	256	RS3

[a] All measured in inches.

(b) Magnification equations

$$\text{CMAG}_{\text{NEW}} = \frac{\text{Calculated magnification}}{\text{MAG}} \times \text{CMAG}_{\text{OLD}}$$

where

$$\text{Calculated magnification} = 256 \frac{(F1)(F2)}{-(FA0)^2 + FA0(L1 - F1) + F2(L1 - F1)}$$

TABLE AII. FIXATION PLANE CONSTANTS

[All distances measured in inches]

(a) Fixation plane origin offsets with respect to oculometer axis system

$$X0 = 256 \times (X\text{-axis offset})$$
$$Y0 = 256 \times (Y\text{-axis offset})$$
$$Z0 = 256 \times (Z\text{-axis offset})$$

(b) Mirror box pitch-up

$$D1 = 16\,384 \times \sin(\text{Pitch-up angle})$$
$$D2 = 16\,384 \times \cos(\text{Pitch-up angle})$$

(c) Direction cosines of fixation plane

X-axis: $\quad Q1 = 1024 \; \cos\psi\cos\theta$
$\quad\quad\quad M1 = 1024 \; (\cos\psi\sin\theta\sin\phi - \sin\psi\cos\phi)$
$\quad\quad\quad N1 = 1024 \; (\cos\psi\sin\theta\sin\phi + \sin\psi\cos\phi)$

Y-axis: $\quad Q2 = 1024 \; \sin\psi\cos\theta$
$\quad\quad\quad M2 = 1024 \; (\sin\psi\sin\theta\sin\phi + \cos\psi\cos\phi)$
$\quad\quad\quad N2 = 1024 \; (\sin\psi\sin\theta\cos\phi - \cos\psi\sin\phi)$

Normal: $\quad L3 = -1024 \; \sin\theta$
$\quad\quad\quad M3 = 1024 \; \cos\theta\sin\phi$
$\quad\quad\quad N3 = 1024 \; \cos\theta\cos\phi$

where

$\psi = $ Roll angle
$\theta = $ Yaw angle
$\phi = $ Pitch angle

(d) Scale factors

$$\text{SCFX2} = 6554 \times (\text{Volts per horizontal inch on instrument panel})$$
$$\text{SCFY2} = 6554 \times (\text{Volts per vertical inch on instrument panel})$$

(e) Location of zero-volt output from x and y data channels

$$\text{DDX} = \frac{\text{SCFX2}}{64} \times (\text{Horizontal distance from reference point to zero-volt } x\text{-channel output})$$
$$\text{DDY} = \frac{\text{SCFY2}}{64} \times (\text{Vertical distance from reference point to zero-volt } y\text{-channel output})$$

TABLE AII. Concluded

(f) Calibration points

$$\text{CALX} = 16 \times (\text{Distance from reference point to horizontal calibration point})$$
$$\text{CALY} = 16 \times (\text{Distance from reference point to vertical calibration point})$$

(g) Ideal points

$$(\text{TX})_n = 8192 \times \frac{(\text{Horizontal distance from reference point to center of instrument n})}{(\text{Distance from horizontal reference point to calibration point})}$$
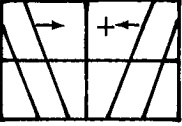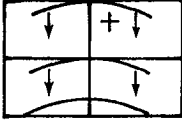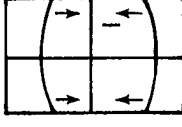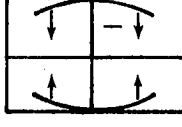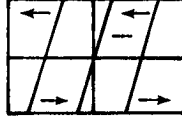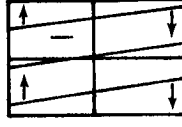
$$(\text{TY})_n = 8192 \times \frac{(\text{Vertical distance from reference point to center of instrument n})}{(\text{Distance from vertical reference point to calibration point})}$$

(h) Home base point

$$\text{XCNTR} = \left[\frac{\text{SCFX2}}{64} \times (\text{Horizontal distance from reference point to home base point})\right] + \text{DDX}$$

$$\text{YCNTR} = \left[\frac{\text{SCFY2}}{64} \times (\text{Vertical distance from reference point to home base point})\right] + \text{DDY}$$

TABLE AIII. LINEARIZATION COEFFICIENTS

Distortion	Sensitivity, machine value change for 1° effect	Symbol
	100	KX
	50	KY
	200	AKX
	200	AKY
	40	BKX
	25	BKY
X gain (+ decreases gain)	250	J1
Y gain (+ decreases gain)	200	J2
X gain (one side; + increases gain)	250	J4L
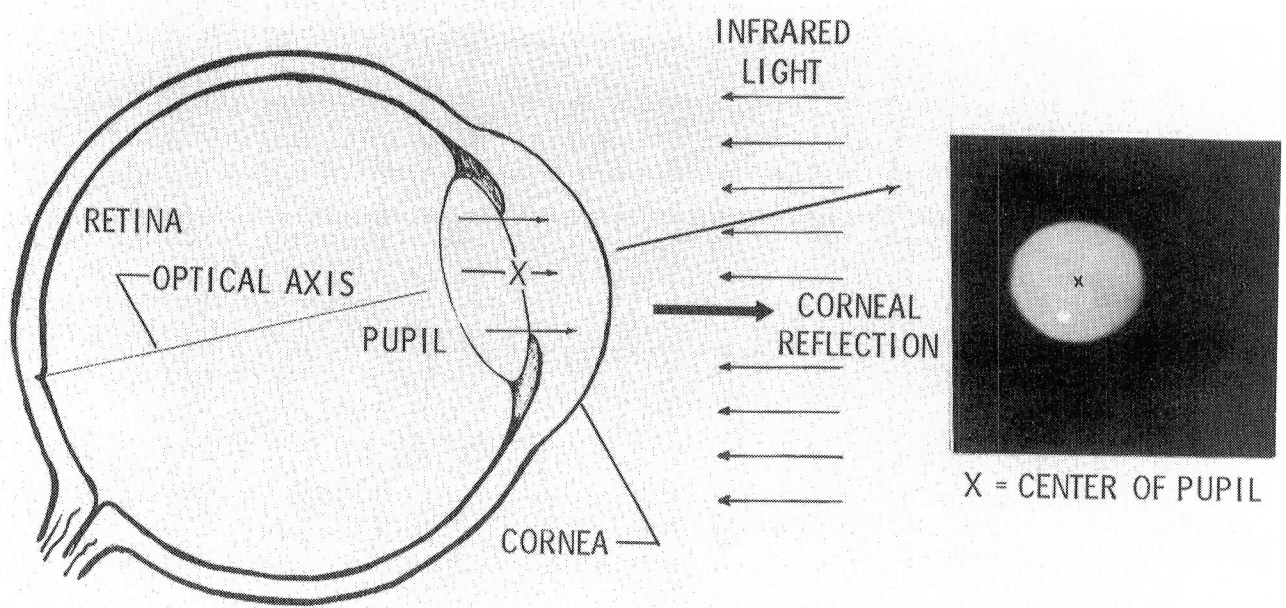
Figure A1. Basic sensing principle.

Electro-optic head

L-74-2679
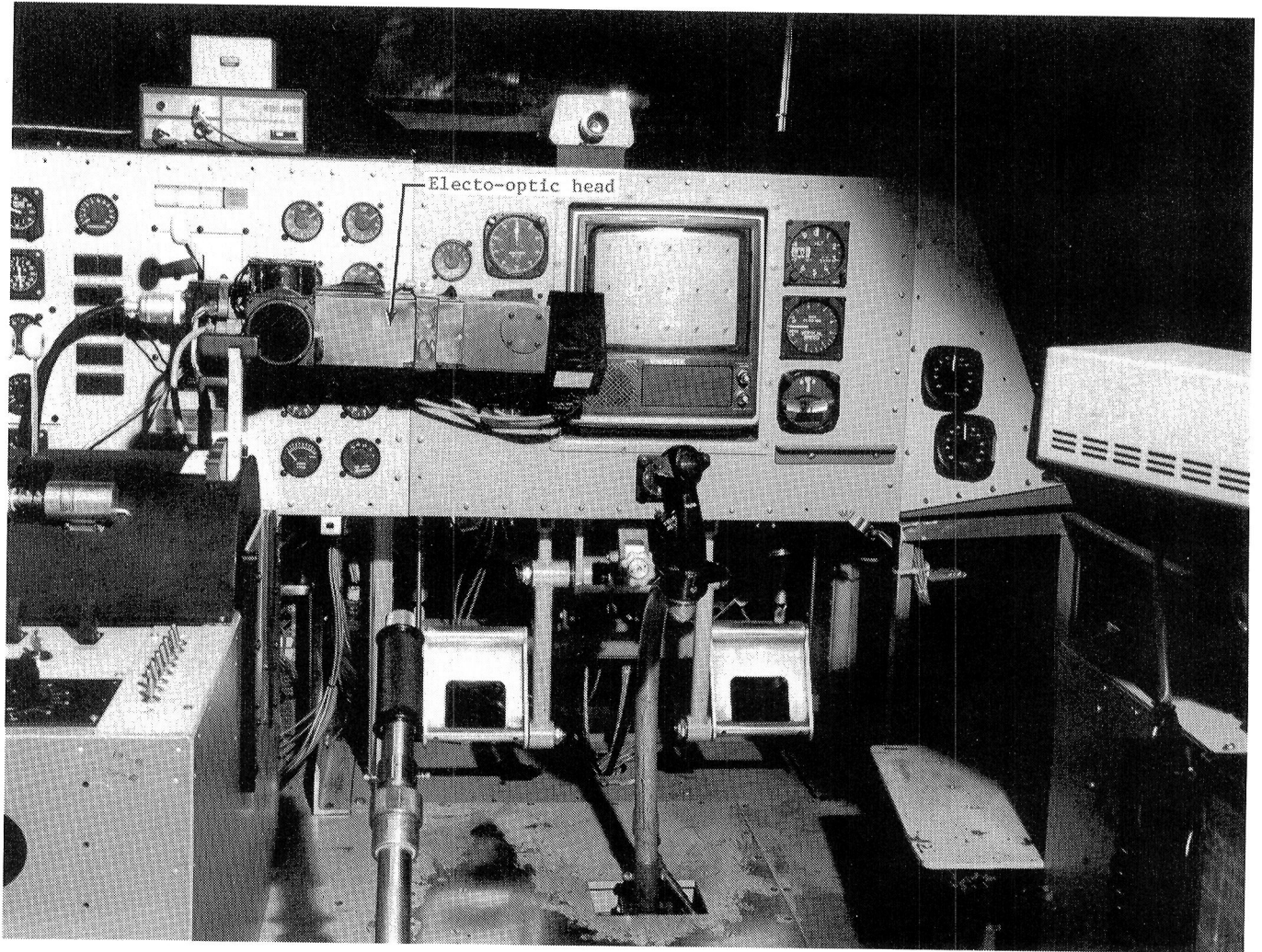
Figure A2. Honeywell electro-optic head.

Electo-optic head

Figure A3. Modified electro-optic head.

L-78-2234
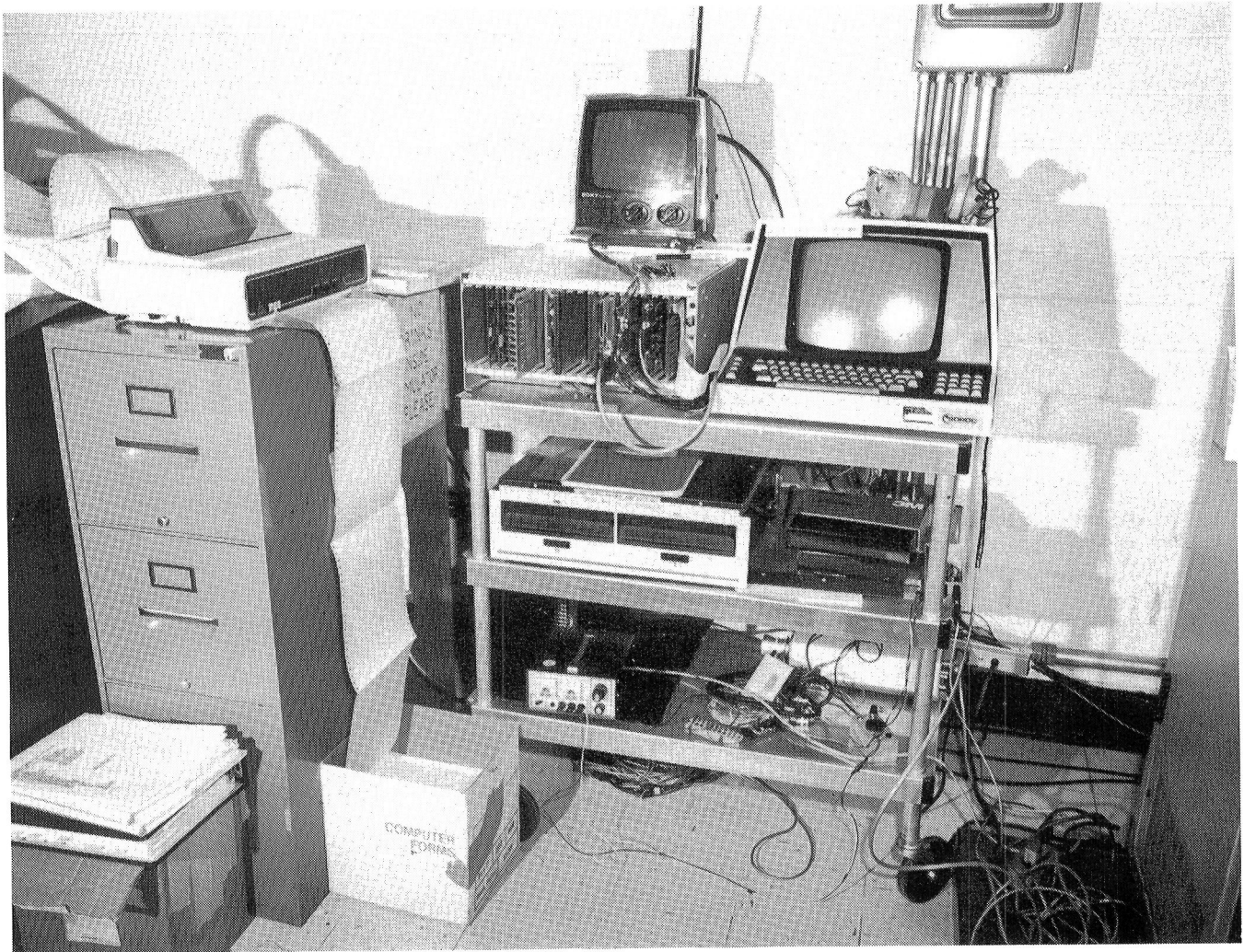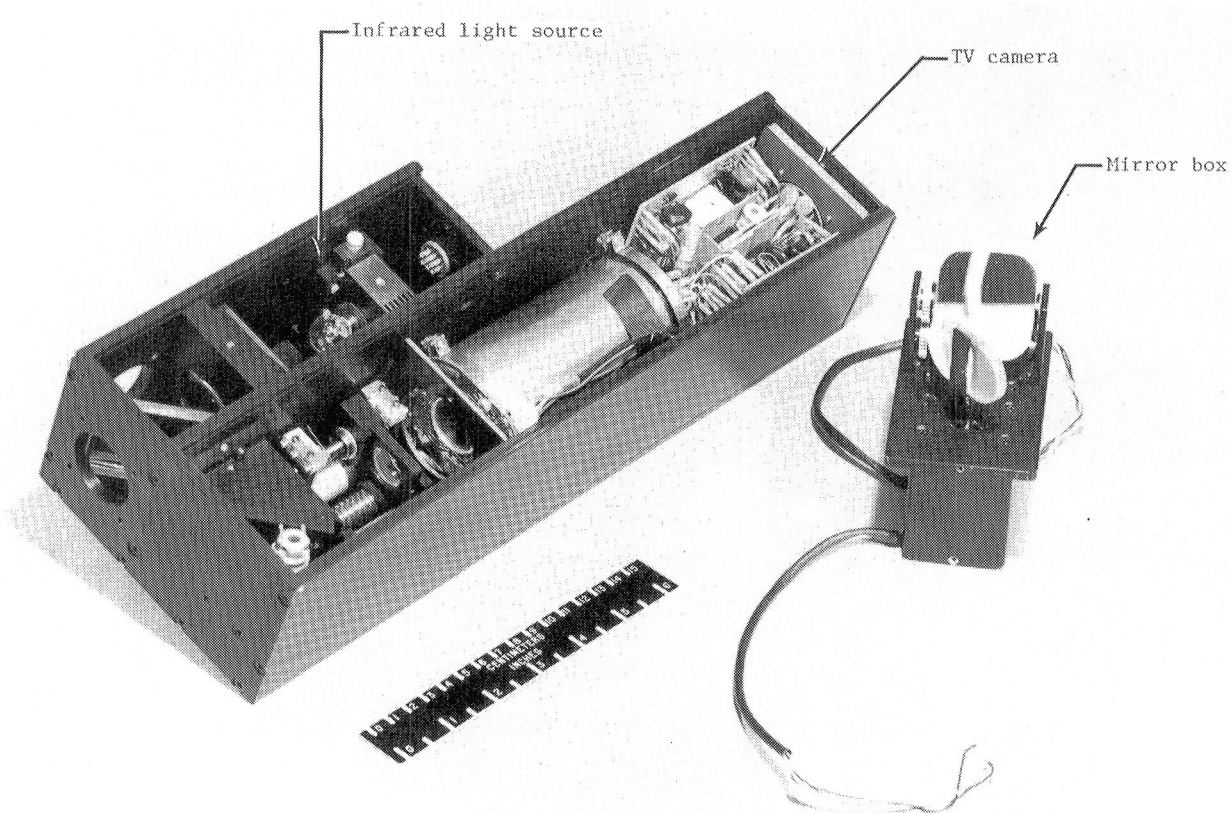
Figure A4. Microprocessor-based data collection system.

Infrared light source
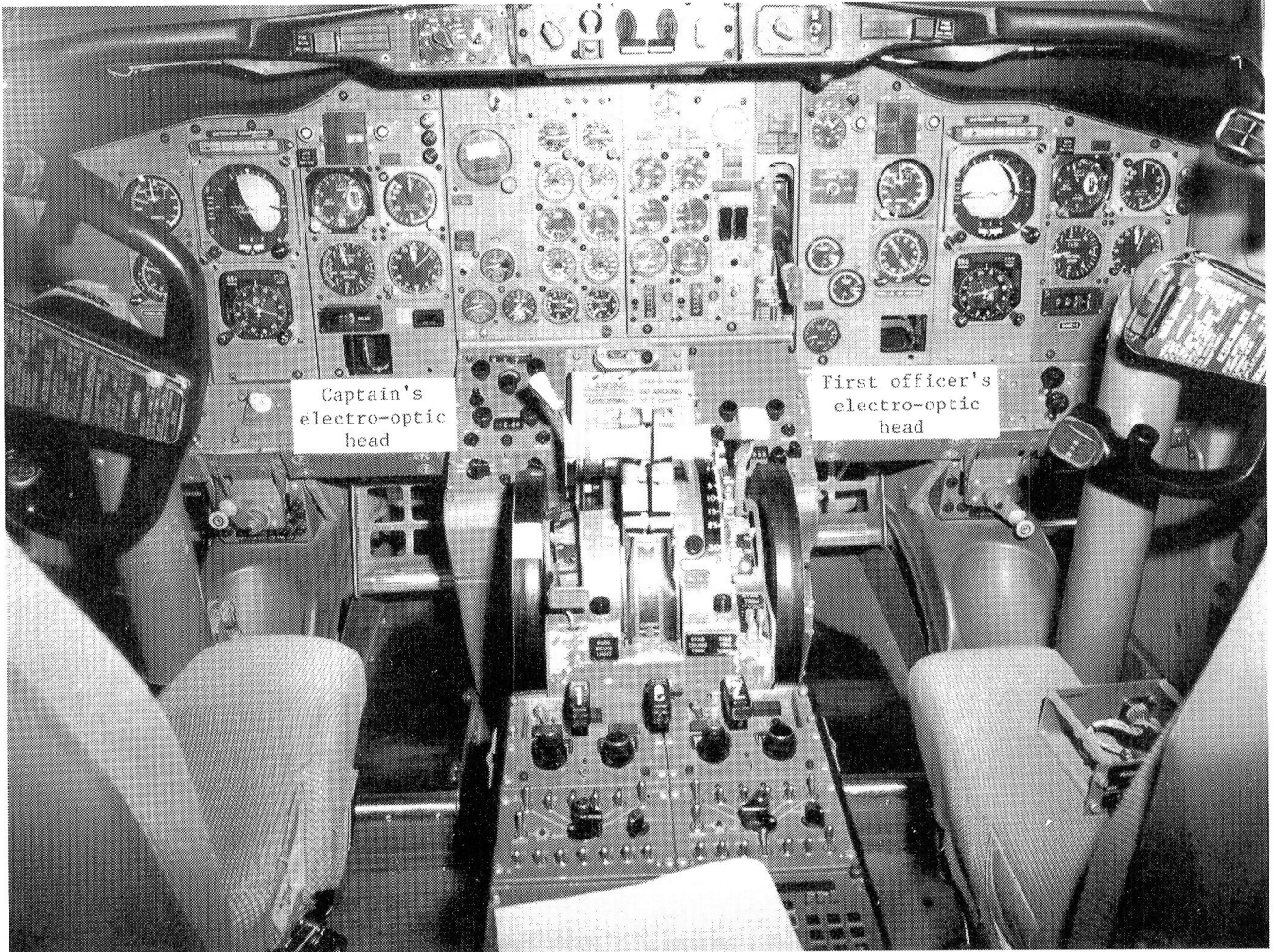
TV camera

Mirror box

Figure A5. Current electro-optic head.

L-79-4906

Figure A6. Current electro-optic heads installed in cockpit.

L-82-5257

Appendix B

Overview of Data Reduction

The primary data reduction effort for oculometric studies involves the use of three programs: SCAN, SUMMARY, and HISTO. These programs were developed specifically to enhance oculometer data reduction.

Functional Description of Program SCAN

Program SCAN calculates raw scanning-behavior parameters. It is by far the most important of the three primary oculometric programs, since it creates files to be used by the other programs and provides an initial detailed analysis of oculometric data. Figure B1 presents a very simplified flowchart of program SCAN which can be referred to in the following discussion. SCAN's input is simple and consists of flag settings to control program options, instrument boundary coordinates, and binary-coded data file(s) containing time histories of oculometric and other data (generally aircraft state and performance data). The output is a comprehensive first look at scanning-behavior data for each individual run and includes lookpoint (Markov) transition matrices, histograms of dwell time occurrences versus length of occurrence for each instrument, counts of the number of control inputs made by the pilot, means and standard deviations of instrument dwell times, state and performance variables, and other single-variable-statistics. SCAN also outputs two ASCII coded files, one used by program SUMMARY and the other by program HISTO. The file for SUMMARY is a compilation of the single-run output statistics of SCAN. The file for HISTO contains a sequential listing of the instrument number, the length of the fixation, and the number and timing of control events (if any) which occurred during that fixation. Special purpose modifications to SCAN have been made in the past to recreate graphic displays for determining at which individual element of the graphic display information the pilot was looking.

Functional Description of Program Summary

Program SUMMARY, as the name implies (see fig. B2), combines and summarizes most of the single-run statistics that are output by SCAN. That is, after a complete data set is finished, SUMMARY can be executed with the multiple-run files from SCAN to provide a data set summation. In addition to the summation of SCAN information, SUMMARY also performs the necessary computations required for t tests and F ratios on instrument scanning-behavior parameters and aircraft state and performance variables. The statistical comparisons are controlled by user input flags and include pilot versus pilot, condition versus condition, and pilot versus condition. A maximum of six comparisons can be made in a single execution. The output of SUMMARY consists of four tables. Each table is a listing of the calculated statistics for each of the up-to-six comparisons for all the scanning-behavior data and the aircraft state and performance variables. The first table contains the F ratios, the second table contains the variances, the third table contains the t statistics and degrees of freedom, and the fourth table contains the means.

Functional Description of Program HISTO

Program HISTO calculates dwell time distributions. It is executed with the file(s) of fixation times and control input event times from program SCAN. Figure B3 illustrates the basic operations performed to obtain the dwell histograms. HISTO reduces these data into dwell time histograms. Six tables are produced with the data. The first four are dwell time histograms, and the last two are fixations/dwell histograms. The first histogram represents the number of times that a subject's dwell length during control inputs lasted a designated time for a given instrument. The second converts the counts of the first histogram to a percentage with respect to total counts for that particular instrument. The third and fourth histograms differ from the first two only in that no control input was made during these dwells. The fifth and sixth histograms depict the number of fixations per dwell for a given instrument with and without control inputs, respectively. HISTO can be modified to output fixation histograms instead of dwell histograms, since the data file contains fixation counts. Special purpose modifications might include histograms of the time from the beginning of a dwell/fixation to a control input or histograms of the time from a control input to the end of a dwell/fixation.
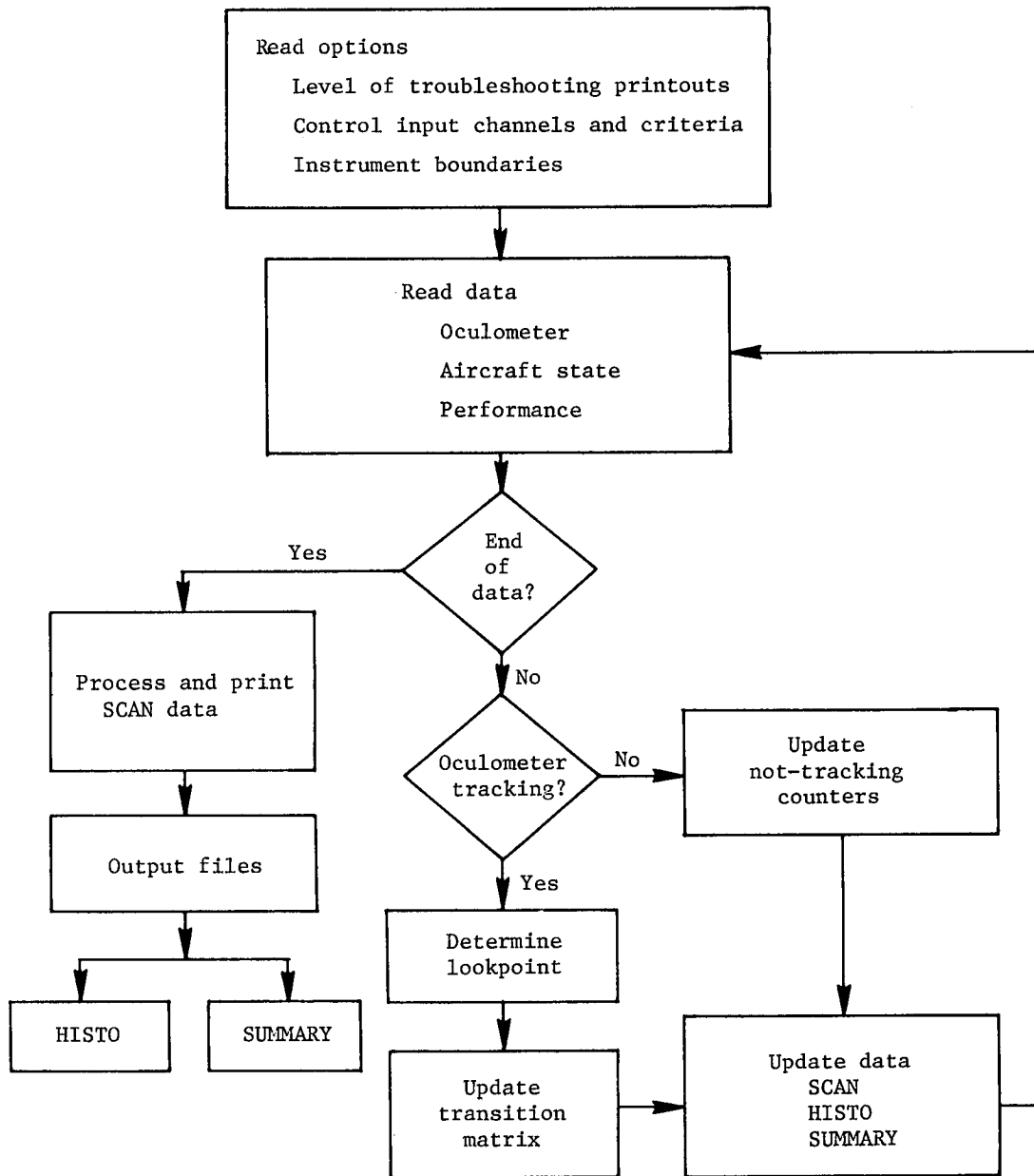
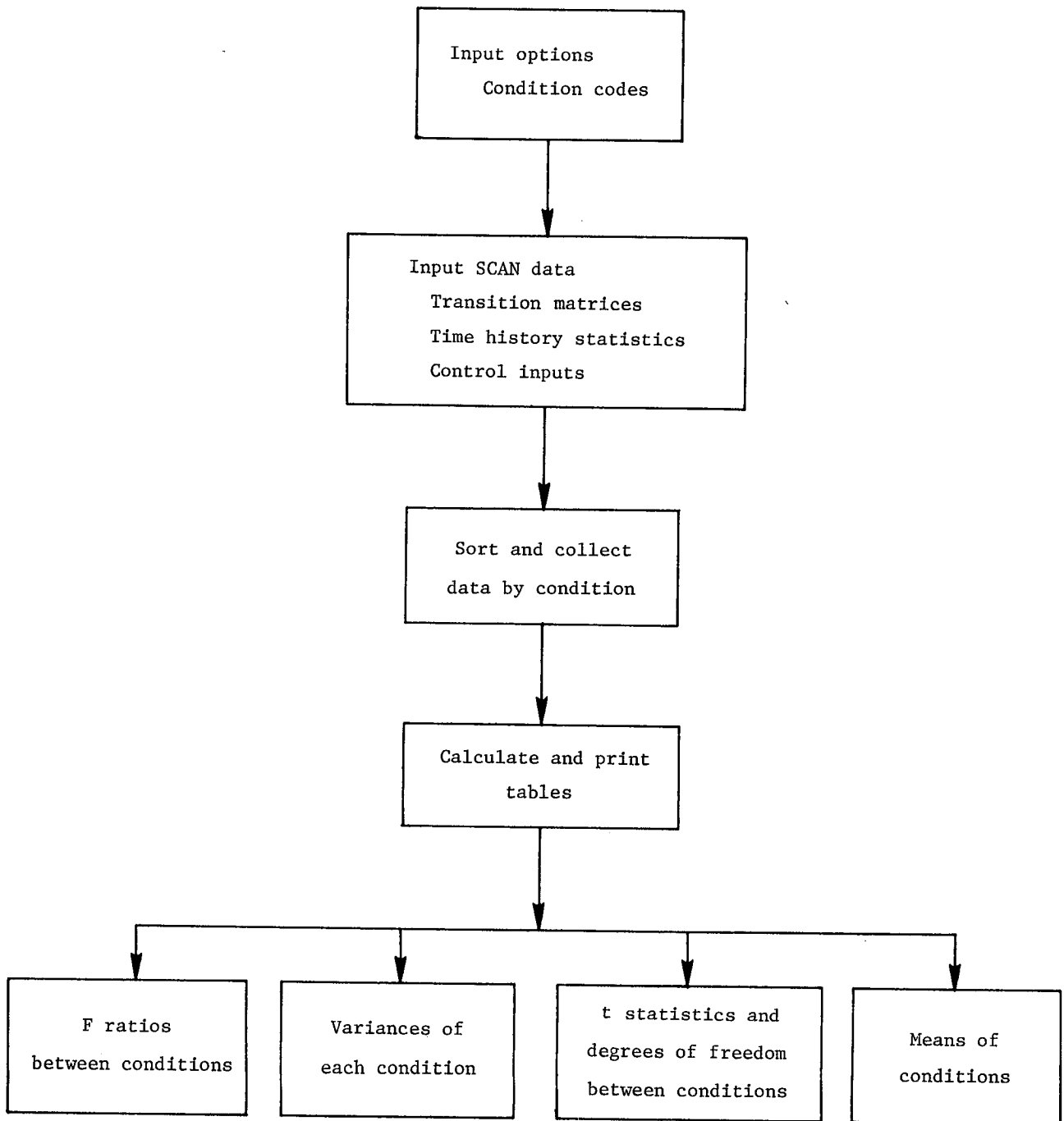Figure B1. Flowchart of SCAN computer program.

Figure B2. Flowchart of SUMMARY computer program.

```
                    ┌─────────────────────────┐
                    │   Input data            │
                    │      Instrument fixated  │
                    │      Fixation length     │
                    │      Control inputs      │
                    └─────────────────────────┘
```

Input data
  Instrument fixated
  Fixation length
  Control inputs

Sort and collect
  data by
dwell (or fixation) length
and pilot's control activity

Calculate and print
histogram tables

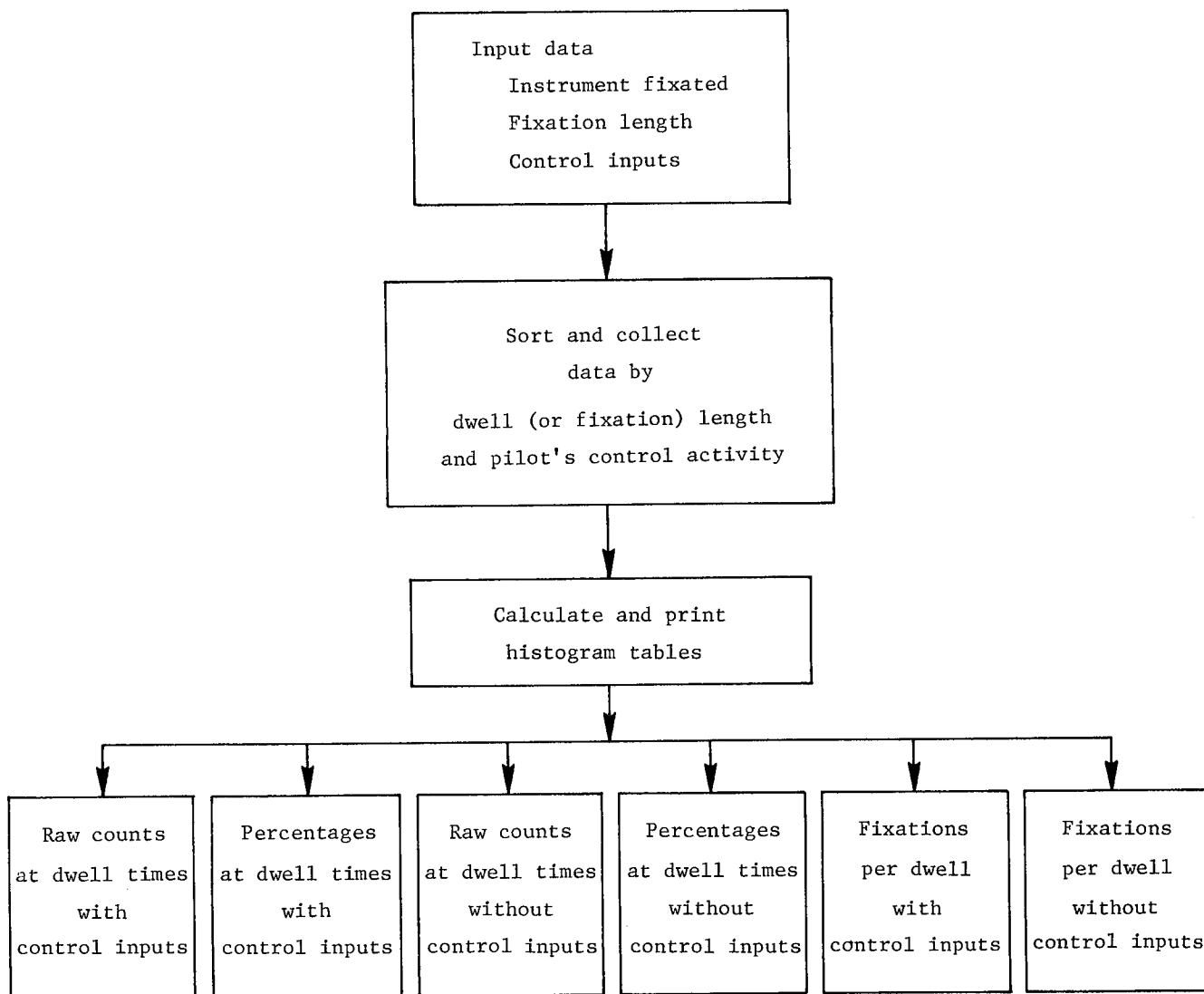| Raw counts at dwell times with control inputs | Percentages at dwell times with control inputs | Raw counts at dwell times without control inputs | Percentages at dwell times without control inputs | Fixations per dwell with control inputs | Fixations per dwell without control inputs |

Figure B3. Flowchart of HISTO computer program.

Appendix C

Glossary

Average dwell time The total time spent looking at an instrument divided by the total number of individual dwells on that instrument.

Dwell percentage Dwell time on a particular instrument as a percent of total scanning time.

Dwell time The time spent looking within the boundary of an instrument.

Fixation A series of continuous lookpoints which stay within a radius of 1 visual degree.

Fixations per dwell The number of individual fixations during an instrument dwell.

Lookpoint The current coordinates of where the pilot is looking during any one thirtieth of a second.

Oculometer A device which measures the lookpoint of a test subject.

One-way transition The sum of all transitions from one instrument to another (one direction only) in a specified instrument pair.

Out of track A state in which the oculometer cannot determine where the pilot is looking, such as during a blink or when the subject's head movement has exceeded the tracking capabilities of the oculometer.

Saccade The spatial change in fixations.

Scan Eye movement technique used to accomplish a given task. Measures used to quantify a scan include (but are not limited to) transitions, dwell percentages, and average dwell times.

Transition The change of a dwell from one instrument to another.

Transition Rate The number of transitions per second.

Two-way transition The sum of all transitions between an instrument pair, regardless of direction of the transition.

Appendix D

Bibliography of LaRC-Sponsored Research on Pilot Scanning Behavior

Comstock, James R., Jr.: The Effects of Simulator and Aircraft Motion on Eye Scan Behavior. *Proceedings of the Human Factors Society 28th Annual Meeting*, Mary Jane Alluisi, Sybil de Groot, and Earl A. Alluisi, eds., Volume 1, Human Factors Soc., Inc., c.1984, pp. 128–132.

Comstock, James R., Jr.: *Oculometric Indices of Simulator and Aircraft Motion*. NASA CR-3801, 1984.

Comstock, James R., Jr.; Coates, Glynn D.; and Kirby, Raymond H.: Eye-Scan Behavior in a Flight Simulation Task as a Function of Level of Training. *Proceedings of the Human Factors Society 29th Annual Meeting*, Robert W. Swezey, ed., Volume I, c.1985, Human Factors Soc., Inc., pp. 391–395.

Dick, A. O.: *Double-Cross Validation of Eye Scan Measurements Obtained During Simulator Landing*. Tech. Rep. No. 1-77 (NASA Grant NSG-1211), Behavioral Research Applications Group, Inc., 1977. (Available as NASA CR-149890.)

Dick, A. O.: An Evaluation of Eye Scanning on Instruments During Landing. Paper presented at Air Line Pilots Association Symposium on Human Factors Emphasizing Human Performance Workload and Communications (Washington, D.C.), Feb. 8, 1977.

Dick, A. O.: *Instrument Scanning and Controlling: Using Eye Movement Data To Understand Pilot Behavior and Strategies*. NASA CR-3306, 1980.

Dick, A. O.; Brown, John Lott; and Bailey, George: *Statistical Evaluation of Control Inputs and Eye Movements in the Use of Instrument Clusters During Aircraft Landing*. TR-4-76 (NASA Grant NSG-1211), Center for Visual Science, Univ. of Rochester, [1977]. (Available as NASA CR-149465.)

Ephrath, A. R.; Tole, J. R.; Stephens, A. T.; and Young, L. R.: Instrument Scan - Is It an Indicator of the Pilot's Workload? *Proceedings of the Human Factors Society 24th Annual Meeting, Human Factors: Science for Working and Living*, George E. Corrick, Eric C. Haseltine, and Robert T. Durst, Jr., eds., 1980, pp. 257–258.

Fulton, C. L.; and Harris, R. L., Sr.: *Error Analysis and Corrections to Pupil Diameter Measurements With Langley Research Center's Oculometer*. NASA TM-81806, 1980.

Gainer, Patrick A.: Analysis of Visual Estimation of System State From Arbitrary Displays. *Models of Human Operators in Visual Dependent Tasks*, Marvin C. Waller, ed., NASA CP-2103, 1979, pp. 61–82.

Galanter, Eugene; and Hochberg, Julian: Behavioral Indicators of Pilot Workload. *Proceedings of the Second Symposium on Aviation Psychology*, R. S. Jensen, ed., Ohio State Univ. Dept. of Aviation, 1983, pp. 243–252.

Galanter, Eugene; and Popper, Richard: *Development and Evaluation of a General Aviation Real World Noise Simulator*. NASA CR-159237, 1980.

Goode, Plesent W.: Eye Directed View. *New Opportunities in Space, Proceedings of Twenty-First Space Congress*, Canaveral Council Tech. Soc., 1984, pp. 2-1–2-15.

Guy, Warren J.: *Oculometer Focus and Mirror Control*. NASA CR-166007, 1982.

Harris, Randall L., Sr.: *Preliminary Investigation of Pilot Scanning Techniques of Dial Pointing Instruments*. NASA TM-80079, 1979.

Harris, Randall L., Sr.: Effects of Foveal Information Processing. *Peripheral Vision Horizon Display (PVHD)*, NASA CP-2306, 1984, pp. 81–88.

Harris, Randall L., Sr.; and Christhilf, David M.: What Do Pilots See in Displays? *Proceedings of the Human Factors Society 24th Annual Meeting, Human Factors: Science for Working and Living*, George E. Corrick, Eric C. Haseltine, and Robert T. Durst, Jr., eds., 1980, pp. 22–26.

Harris, Randall L., Sr.; and Glover, Bobby J.: Effects of Digital Altimetry on Pilot Workload. Paper presented at the 1984 SAE Aerospace Congress & Exposition (Long Beach, Calif.), Oct. 15–18, 1984.

Harris, Randall L., Sr.; and Mixon, Randolph W.: Advanced Transport Operation Effects on Pilot Scan Patterns. *Proceedings of the Human Factors Society 23rd Annual Meeting*, Carolyn K. Bensel, ed., 1979, pp. 347–351.

Harris, Randall L., Sr.; and Mixon, Randolph W.: *Effects of Curved Approach Paths and Advanced Displays on Pilot Scan Patterns*. NASA TP-1846, 1981.

Harris, Randall L., Sr.; and Spady, Amos A., Jr.: Visual Scanning Behavior. *IEEE 1985 National Aerospace and Electronics Conference— NAECON 1985*, Volume 2, 85CH2189-9, 1985, pp. 1032–1039.

Harris, Randall L., Sr.; Tole, John R.; Ephrath, Arye R.; and Stephens, A. Thomas: How a New Instrument Affects Pilots' Mental Workload. *Proceedings of the Human Factors Society 26th Annual Meeting*, Richard E. Edwards, ed., 1982, pp. 1010–1013.

Harris, R. L., Sr.; Tole, J. R.; Stephens, A. T.; and Ephrath, A. R.: Visual Scanning Behavior and Pilot Workload. *Proceedings of the First Symposium on Aviation Psychology*, Ohio State Univ. Aviat. Psychology Lab., 1981, pp. 216–225.

Harris, R. L., Sr.; Tole, J. R.; Stephens, A. T.; and Ephrath, A. R.: Visual Scanning Behavior and Pilot Workload. *Aviat., Space & Environ. Med.*, vol. 53, no. 11, Nov. 1982, pp. 1067–1072.

Harris, R. L., Sr.; Waller, M. C.; and Salmirs, S.: Runway Texturing Requirements for a Head-Down Cathode Ray Tube Approach and Landing Display. AIAA Paper No. 78-1588, Sept. 1978.

Jones, Dennis H.: *An Error-Dependent Model of Instrument-Scanning Behavior in Commercial Airline Pilots.* NASA CR-3908, 1985.

Jones, Dennis H.; Coates, Glynn D.; and Kirby, Raymond H.: *The Effectiveness of an Oculometer Training Tape on Pilot and Copilot Trainees in a Commercial Flight Training Program.* NASA CR-3666, 1983.

Jones, Dennis H.; Coates, Glynn D.; and Kirby, Raymond H.: *The Effectiveness of Incorporating a Real-Time Oculometer System in a Commercial Flight Training Program.* NASA CR-3667, 1983.

Karmarkar, J. S.; and Sorensen, J. A.: *Information and Display Requirements for Independent Landing Monitors.* NASA CR-2687, 1976.

Krebs, Marjorie J.; and Wingert, James W.: *Use of the Oculometer in Pilot Workload Measurement.* NASA CR-144951, 1976.

Krebs, Marjorie J.; Wingert, James W.; and Cunningham, Thomas: *Exploration of an Oculometer-Based Model of Pilot Workload.* NASA CR-145153, 1977.

Livingston, David L.: A High Speed Algorithmic Processor for Signal Processing Applications. M. Eng. Thesis, Old Dominion Univ., Aug. 1978.

Middleton, D. B.; Hurt, G. J., Jr.; Wise, M. A.; and Holt, J. D.: *Preliminary Flight Tests of an Oculometer.* NASA TM X-72621, 1974.

Middleton, David B.; Hurt, George J., Jr.; Wise, Marion A.; and Holt, James D.: *Description and Flight Tests of an Oculometer.* NASA TN D-8419, 1977.

Miller, K. H.: *Timeline Analysis Program (TLA-1) Final Report.* NASA CR-144942, 1976.

Mout, Michael L.; and Burgin, George H.: *A Computer Program for the Use of Sensitivity Analysis in Display Evaluation.* NASA CR-145060, [1976].

Mout, Michael L.; Burgin, George H.; and Walsh, Michael J.: *Use of Sensitivity Analysis To Predict Pilot Performance as a Function of Different Displays.* NASA CR-2906, 1977.

North, R. A.; Stackhouse, S. P.; and Graffunder, K.: *Performance, Physiological, and Oculometer Evaluation of VTOL Landing Displays.* NASA CR-3171, 1979.

Pennington, Jack E.: *Single Pilot Scanning Behavior in Simulated Instrument Flight.* NASA TM-80178, 1979.

Spady, Amos A., Jr.: Airline Pilot Scanning Behavior During Approaches and Landing in a Boeing 737 Simulator. *Guidance and Control Design Considerations for Low-Altitude and Terminal-Area Flight,* AGARD-CP-240, Apr. 1978, pp. 17-1–17-5.

Spady, Amos A., Jr.: *Airline Pilot Scan Patterns During Simulated ILS Approaches.* NASA TP-1250, 1978.

Spady, Amos A., Jr.; and Harris, Randall L., Sr.: How a Pilot Looks at Altitude. *1980 Aircraft Safety and Operating Problems,* Joseph W. Stickle, compiler, NASA CP-2170, Pt. 1, 1981, pp. 237-248. (Available as NASA TM-81967.)

Spady, Amos A., Jr.; and Harris, Randall L., Sr.: Summary of NASA Langley's Pilot Scan Behavior Research. *Second Aerospace Behavorial Engineering Technology Conference Proceedings,* P-132, Soc. Automot. Eng., Inc., 1983, pp. 91-99. (Available as SAE Paper 831424.)

Spady, Amos A., Jr.; Harris, Randall L., Sr.; and Comstock, Raymond: Flight Versus Simulator Scan Behavior. *Proceedings of the Second Symposium on Aviation Psychology,* R. S. Jensen, ed., Ohio State Univ. Dep. Aviation, 1983, pp. 123–130.

Spady, Amos A., Jr.; Jones, Dennis H.; Coates, Glynn D.; and Kirby, Raymond H.: The Effectiveness of Using Real-Time Eye Scanning Information for Pilot Training. *Proceedings of the Human Factors Society 26th Annual Meeting,* Richard E. Edwards, ed., 1982, pp. 1014–1017.

Spady, A. A., Jr.; and Kurbjun, M. C.: Flight Management Research Utilizing an Oculometer—Pilot Scanning Behavior During Simulated Approach and Landing. Paper presented at SAE Air Transportation Meeting (Boston, Mass.), May 1978.

Spady, Amos A., Jr.; and Waller, Marvin C.: The Oculometer, a New Approach to Flight Management Research. AIAA Paper No. 73-914, Sept. 1973.

Stephens, A. T.; Tole, J. R.; Ephrath, A.; and Young, L. R.: Pilot Eye Scanning Behavior as an Index of Mental Loading. MIT paper presented at the 8th Annual Northeast Bioengineering Conference (Cambridge, Mass.), Mar. 1980.

Sundstrom, James L.: *NASA TLA Workload Analysis Support. Volume 1—Detailed Task Scenarios for General Aviation and Metering and Spacing Studies.* NASA CR-3199, 1980.

Sundstrom, James L.: *NASA TLA Workload Analysis Support. Volume 2—Metering and Spacing Studies Validation Data.* NASA CR-3239, 1980.

Sundstrom, James L.: *NASA TLA Workload Analysis Support. Volume 3—FFD Autopilot Scenario Validation Data.* NASA CR-3240, 1980.

Tole, J. R.; Ephrath, A.; Stephens, A. T.; and Young, L. R.: Workload and Pilot Eye Scanning Behavior. *Proceedings of the Sixteenth Annual Conference on Manual Control,* May 1980, p. 214.

Tole, J. R.; Stephens, A. T.; Harris, R. L., Sr.; and Ephrath, A.: Quantification of Pilot Workload Via Instrument Scan. Paper presented at AIAA Workshop on Flight Testing To Identify Pilot Workload and Pilot Dynamics, Jan. 1982. (Available as NASA CR-169238.)

Tole, J. R.; Stephens, A. T.; Harris, R. L., Sr.; and Ephrath, A. R.: Visual Scanning Behavior and Mental Workload in Aircraft Pilots. *Aviat., Space & Environ. Med.,* vol. 53, no. 1, Jan. 1982, pp. 54–61.

Tole, J. R.; Stephens, A. T.; Vivaudou, M.; Ephrath, A.; and Young, L. R.: *Visual Scanning Behavior and Pilot Workload.* NASA CR-3717, 1983.

Tole, J. R.; Stephens, A. T.; Vivaudou, M.; Harris, R. L., Sr.; and Ephrath, A.: Entropy, Instrument Scan, and Pilot Workload. IEEE 1982 Proceedings of the International Conference on Cybernetics and Society, 82CH1840-8, 1982, pp. 588–592.

Varanasi, Murali R.: *Feasibility Study of a Microprocessor-Based Oculometer System.* NASA CR-164286, 1981.

Vivaudou, Michel B.: Design and Evaluation of a Communication Interface Controlled by Patterns of Eye Movements. Ph.D. Thesis, Worcester Polytechnic Inst., Aug. 1984.

Waller, Marvin C.: *An Investigation of Correlation Between Pilot Scanning Behavior and Workload Using Stepwise Regression Analysis.* NASA TM X-3344, 1976.

Waller, Marvin C.: Applications of Pilot Scanning Behavior to Integrated Display Research. *Eighth Annual Symposium Proceedings—Flight Test Technology,* Soc. Flight Test Eng., Aug. 1977, pp. 4-1-4-19.

Waller, Marvin C.: Research in Pilot Scanning Behavior. Paper presented at the 50th Annual Convention of the National Technical Association (New York), Aug. 2-5, 1978.

Waller, Marvin C., ed.: *Models of Human Operators in Vision Dependent Tasks.* NASA CP-2103, 1979.

Waller, Marvin C.; and Flowers, Garry S.: Dwell Time Scanning Characteristics of Pilots During a Simulated Instrument Approach. Paper presented at the Eye Movements and Psychological Processes, II Symposium (Monterey, Calif.), Feb. 7-9, 1977.

Waller, Marvin C.; Harris, Randall L., Sr.; and Person, Lee H., Jr.: *Influence of Display and Control Compatibility on Pilot-Induced Oscillations.* NASA TP-1936, 1981.

Waller, Marvin C.; Harris, Randall L., Sr.; and Salmirs, Seymour: An Evaluation of Some Display Parameters for an Advanced Landing Display. Paper presented at the 51st Annual Convention of the National Technical Association (Pittsburgh, Pennsylvania), Aug. 1-4, 1979.

Waller, Marvin C.; Harris, Randall L., Sr.; and Salmirs, Seymour: A Study of Parameters Affecting a Display for Aircraft Instrument Landings. *Proceedings of the Human Factors Society 23rd Annual Meeting,* Carolyn K. Bensel, ed., 1979, pp. 345-346.

Waller, Marvin C.; and Wise, Marion A.: The Oculometer in Flight Management Research. AIAA Paper No. 75-107, Jan. 1975.

Williams, Allen J.; and Harris, Randall L., Sr.: *Factors Affecting Dwell Times on Digital Displays.* NASA TM-86406, 1985.

Standard Bibliographic Page

1. Report No. NASA TP-2525	2. Government Accession No.	3. Recipient's Catalog No.
4. Title and Subtitle Analytical Techniques of Pilot Scanning Behavior and Their Application		5. Report Date July 1986
		6. Performing Organization Code 505-35-13-06
7. Author(s) Randall L. Harris, Sr., Bobby J. Glover, and Amos A. Spady, Jr.		8. Performing Organization Report No. L-15995
9. Performing Organization Name and Address NASA Langley Research Center Hampton, VA 23665-5225		10. Work Unit No.
		11. Contract or Grant No.
12. Sponsoring Agency Name and Address National Aeronautics and Space Administration Washington, DC 20546-0001		13. Type of Report and Period Covered Technical Paper
		14. Sponsoring Agency Code

15. Supplementary Notes

16. Abstract

This report documents the state of the art of oculometric data analysis techniques and their applications in certain research areas such as pilot workload, information transfer provided by various display formats, crew role in automated systems, and pilot training. These analytical techniques produce the following data: real-time viewing of the pilot's scanning behavior, average dwell times, dwell percentages, instrument transition paths, dwell histograms, and entropy rate measures. These types of data are discussed, and overviews of the experimental setup, data analysis techniques, and software are presented. A glossary of terms frequently used in pilot scanning behavior and a bibliography of reports on related research sponsored by NASA Langley Research Center are also presented.

17. Key Words (Suggested by Authors(s)) Pilot scan behavior Workload Oculometer	18. Distribution Statement Unclassified—Unlimited Subject Category 53

19. Security Classif.(of this report) Unclassified	20. Security Classif.(of this page) Unclassified	21. No. of Pages 44	22. Price A03

National Aeronautics and
Space Administration
Code NIT-4

Washington, D.C.
20546-0001

Official Business
Penalty for Private Use, $300
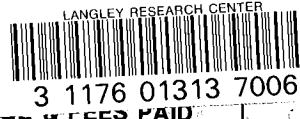
NASA

POSTMASTER: If Undeliverable (Section 158
Postal Manual) Do Not Return